ADVANCED MATERIALS
www.advmat.de

Carbon-Nanomaterial-Based Flexible Batteries for Wearable Electronics

Ziping Wu, Yonglong Wang, Xianbin Liu, Chao Lv, Yesheng Li, Di Wei,* and Zhongfan Liu**

Wearable electronics have received considerable attention in recent years. These devices have penetrated every aspect of our daily lives and stimulated interest in futuristic electronics. Thus, flexible batteries that can be bent or folded are desperately needed, and their electrochemical functions should be maintained stably under the deformation states, given the increasing demands for wearable electronics. Carbon nanomaterials, such as carbon nanotubes, graphene, and/or their composites, as flexible materials exhibit excellent properties that make them suitable for use in flexible batteries. Herein, the most recent progress on flexible batteries using carbon nanomaterials is discussed from the viewpoint of materials fabrication, structure design, and property optimization. Based on the current progress, the existing advantages, challenges, and prospects are outlined and highlighted.

1. Introduction

Electronics have revolutionarily changed our lives since the discovery of transistors seven decades ago.[1] In recent years, portable electronics, such as rolled-up displays, touch screens, smart clothes, and implantable medical devices, have revealed novel applications for future human society and daily life.[2] Intelligent electronics should be flexible, bendable, or naturally foldable for integration with the human body to meet the ubiquitous applications that are considered the next-generation revolution.[3–5] Consequently, flexible or foldable batteries for energy storage should be developed to satisfy the power requirements of wearable electronics. Thus, addressing the challenges for applying shape-conformable batteries that correspond to electronics has become a key prerequisite to realize intelligent wearable electronics.[6]

Lithium-ion batteries (LIBs) are an ideal candidate for the power supply of electronics given their high energy density, working voltage, and cycle life.[7] However, conventional LIBs are typically heavy and rigid, considering their traditional configuration, fabrication methods, and metallic current collectors.[8] Generally, cathode[9] and anode[10] materials are mixed with conductive agents and polymer binders, respectively. Then, the slurries are coated on aluminum and copper foils for electrodes, followed by drying and pressing.[11] Typical full LIBs can be obtained, where the electrodes, separators, and electrolytes are assembled together and then packaged. The active materials of the cathode and anode are easily delaminated from the current collectors considering the poor adhesion the active materials and the metallic current collectors. Thus, traditional LIBs will fail after repeated deformation. In addition, the poor adhesion between the contact interfaces results in poor contact electronic conductivity, and the electrochemical performance of the obtained batteries will be deteriorated.

All the components of the batteries should be deformed to address the aforementioned problems; however, traditional electrodes are insufficiently flexible. Thus, a technology to maximize shape-conformable electrodes for batteries should be developed to realize intelligent wearable electronics.[12] The desired electrodes with deformable features should satisfy the following requirements: i) High interfacial adhesion between the active materials and the current collectors should be obtained. In addition, their durability should be improved when subjected to large deformation cycles in wearable electronic devices. ii) Considerable active materials should be deposited to the current collectors to ensure high mass loading, in which the high energy density of the batteries can be obtained. iii) The above electrodes should maintain a high electrical conductivity for rapidly transferring electrons in full batteries with low internal resistance. Flexible packaging is another significant problem for flexible batteries in addition to the abovementioned factors. Therefore, developing novel approaches for flexible electrodes and packaging materials remain as challenges.[13–15]

Carbon nanomaterials have attracted increasing interest in flexible batteries; examples of these carbon nanomaterials

Dr. Z. Wu, Y. Wang, Dr. X. Liu, C. Lv, Y. Li
School of Materials Science and Engineering
Jiangxi University of Science and Technology
86 Hong Qi Road, Ganzhou 341000, P. R. China
E-mail: wuziping724@jxust.edu.cn
Dr. Z. Wu, Prof. Z. Liu
Center for Nanochemistry
Beijing Science and Engineering Center for Nanocarbons
Beijing National Laboratory for Molecular Sciences
College of Chemistry and Molecular Engineering
Peking University
Beijing 100871, P. R. China
E-mail: zfliu@pku.edu.cn
Dr. D. Wei, Prof. Z. Liu
Beijing Graphene Institute
Beijing 100094, P. R. China
E-mail: weidi-cnc@pku.edu.cn
The ORCID identification number(s) for the author(s) of this article can be found under https://doi.org/10.1002/adma.201800716.

DOI: 10.1002/adma.201800716

are carbon nanotubes (CNTs) and graphene with a special microscopic structure that features low density, high strength, favorable conductivity, and excellent flexibility.[16,17] CNTs are allotropes of carbon with a cylindrical nanostructure, and they have been constructed with a very high length-to-diameter ratio, significantly larger than for any other material. These cylindrical carbon molecules have unusual properties, which are valuable for flexible batteries. Graphene is also a crystalline allotrope of carbon with 2D properties. Its carbon atoms are packed densely in a regular atomic-scale pattern. The structure conducts electricity efficiently and the internal resistance of the whole battery can also be decreased. The porous morphology of the carbon nanomaterials enables the active materials to adhere robustly, thereby possibly mitigating the delamination problem with repeated operation after the batteries are fixed on the body. The obtained strong interface of the electrode will demonstrate high mass loading of active material; thereby, high energy density of the batteries can be fabricated. Recent studies have reported that flexible and foldable supercapacitors and batteries with high power densities and energy densities[18–20] can be worn on the body using carbon-based nanomaterials, such as CNT fibers,[21] CNT films,[22] CNT sponges,[23] or graphene fiber,[24] graphene paper,[25,26] graphene foam,[27] or CNT–graphene composite fibers,[28] films,[29] and many other morphologies.[30] Herein, we emphasize the recent achievements on various types of batteries that are flexible or foldable made for wearable electronic applications based on carbon nanomaterials. The preparation, morphology, and properties of the carbon nanomaterials used in the different types of flexible batteries, including LIBs, lithium–sulfur batteries, lithium–air batteries, and zinc–air batteries, are also summarized. Then, a detailed introduction to the fabrication and properties of carbon nanomaterials with different macroscopic morphologies to construct flexible batteries is presented. In the last section, major challenges, perspectives, and opportunities for flexible batteries are discussed. A brief development that summarizes the main studies of flexible batteries is displayed in **Figure 1**. The CNTs used as current collectors for both the anode and cathode in Figure 1a is a significant study for exploring flexible full batteries. After that, batteries with graphene current collectors have also been studied (Figure 1b). Then, CNTs and CNTs/graphene composites have been investigated for 1D batteries (Figure 1c,d). Based on these aforementioned studies, novel flexible batteries or ultrahigh-energy-density batteries with 1D or 2D structure have been developed (Figure 1e–h). These results indicate the development history of flexible batteries.

2. Carbon Nanomaterials

Carbon nanomaterials occupy an exceptional spot in nanoscience given their intriguing physical, chemical, and mechanical properties; in addition, these carbon nanomaterials are used in many aspects, such as composite materials,[31] nanoscale electronic components,[32] and energy storage or conversion systems.[33] Conjugated carbon nanomaterials cover the areas of CNTs and graphene, and continue to gain attention in wearable electronics and other potential fields. Conjugated carbon nanomaterials with high flexibility and light weight are

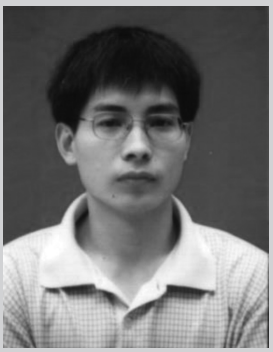

Ziping Wu received his Ph.D. from Shanghai Jiao Tong University in 2010. After that, he became an assistant professor, associate professor (2012), and full professor (2017) of Jiangxi University of Science and Technology. He was a visiting scholar at the Rensselaer Polytechnic Institute in Prof. Koratkar's group from April 2014 to April 2015 and at Peking University in Prof. Zhongfan Liu's group from September 2016 to July 2017. His research interests focus on the preparation of carbon nanomaterials for wearable energy-storage devices and flexible electromagnetic shielding.

Di Wei received his Ph.D. from Abo Akademi University in Finland. After a postdoctoral fellowship at Cambridge University in the UK, he became a senior research scientist at Nokia Technologies Cambridge. He was one of the initiators of the research in the field of nanocarbon and graphene technologies at Nokia. He participated strongly in the early phase of defining and initiating the European Union Graphene Flagship programme during 2011–2013. He became the executive director of the Beijing Graphene Institute in 2017 and holds a fellowship at Wolfson College Cambridge University and adjunct professorship at Abo Akademi University. His research interests cover applications of nanotechnology in sensors and energy devices.

Zhongfan Liu received his Ph.D. from the University of Tokyo in 1990. After a postdoctoral fellowship at the Institute for Molecular Science, Japan, he became an associate professor (1993), full professor (1993), and Cheung Kong Chair professor (1999) of Peking University. He was elected as the member of the Chinese Academy of Science (CAS) in 2011. His research interests focus on low-dimensional carbon materials and novel 2D atomic crystals, targeting nanoelectronic and energy conversion devices together with the exploration of fundamental phenomena in nanoscale systems.

derived from their special microscopic morphology, compared with the widely used traditional metallic current collectors. In addition, the porous structure in carbonaceous nanomaterials results in high mass loading of active materials and strong adhesion of electrodes, by which high energy density in batteries can be obtained.[13] Moreover, the high chemical stability and mechanical strength of carbonaceous nanomaterials result in favorable cyclic reversibility and anticorrosive performance.

CNTs are crystalline allotropes of carbon molecules with a cylindrical structure, and have unusual properties, which are valuable for flexible batteries and electronics.[34] In addition, CNTs have been applied to many smart electronic concepts[35] due to their extraordinary electrical and excellent mechanical properties. Graphene is another crystalline allotrope of carbon; this material consists of a single layer of carbon atoms that are arranged in a hexagonal lattice.[36] Graphene is possibly the newest among the types of carbon nanomaterials and promises to be an active material in the field of flexible batteries and electronics.[37] The corresponding high charge-carrier mobility, robust mechanical properties, and ultrahigh specific surface area of graphene could improve the electrochemical performance and mechanical flexibility of batteries.[38] These applications of carbon nanomaterials benefit from the possibility that they can be fabricated into different uniform macroscopic structures. For example, batteries with a unique 1D cable structure that can be deformable in all dimensions benefit from the excellent wearability of carbon nanomaterial fibers, and batteries with 2D planar structure have good flexibility and high energy density due to flexibility and light weight of carbon-nanomaterial films. Here, we have summarized the recent progress in the preparation approaches, improved properties, and related applications of the corresponding carbon nanomaterials, such as CNTs, graphene, and their composites with different macroscopic morphologies.

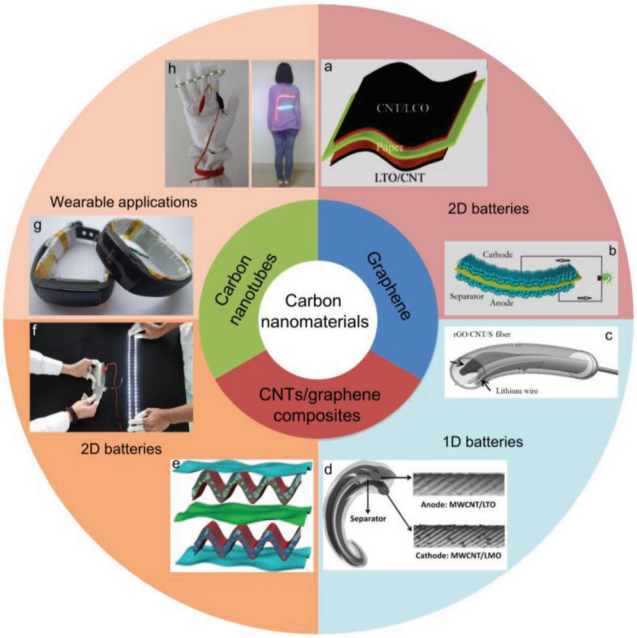

Figure 1. A brief development of flexible batteries based on carbon nanomaterials. Images reproduced with permission as follows: "Thin, flexible secondary Li-ion paper batteries": Reproduced with permission.[98] Copyright 2010, American Chemical Society. "Flexible graphene-based lithium-ion batteries with ultrafast charge and discharge rates": Reproduced with permission.[147] Copyright 2012, National Academy of Sciences USA. "Lithium–sulfur battery cable made from ultralight, flexible graphene/carbon nanotube/sulfur composite fibers:" Reproduced with permission.[119] Copyright 2017, Wiley-VCH. "Elastic and wearable wire-shaped lithium-ion battery with high electrochemical performance:" Reproduced with permission.[111] Copyright 2015, Wiley-VCH. "Gum-like lithium-ion battery based on a novel arched structure:" Reproduced with permission.[107] Copyright 2015, Wiley-VCH. "Potential threshold of anode materials for foldable lithium-ion batteries featuring carbon nanotube current collectors:" Reproduced with permission.[14] Copyright 2016, Elsevier. "Engineering the surface/interface of horizontally oriented carbon nanotube macrofilm for foldable lithium-ion battery withstanding variable weather:" Reproduced with permission.[134] Copyright 2015, Wiley-VCH. "Ultrahigh-energy-density lithium-ion cable battery based on carbon-nanotube woven macrofilms:" Reproduced with permission.[116] Copyright 2017, Wiley-VCH.

2.1. CNTs with Different Macroscopic Morphologies

Owing to the ultrahigh length-to-diameter ratio and covalent sp^2 C—C bonds, CNT bundles with a small diameter are constantly presented as entangled or paralleled.[39] This result shows that fiber, film, or sponge macroscopic morphologies made from CNTs can be easily fabricated. Furthermore, the structure indicates the negligible weight and excellent flexibility of CNTs with 1D, 2D, and 3D macroscopic morphologies.

CNT fibers are first prepared by wet spinning.[40,41] In this process, the as-prepared CNTs are dissolved or dispersed into a fluid, released from a spinneret, and coagulated into a solid fiber by extracting the dispersant. The method is easily scaled to the industrial level. However, an important variation of the original wet-spinning method is by using acid or surfactants as the solvent, thereby resulting in inadequate mechanical strength. CNT fibers can also be drawn and twisted from vertically aligned arrays. An innovation was achieved in 2002[42] and 2004[43] in which CNT yarns were fabricated by directly drawing CNTs from superaligned CNT arrays, shown in **Figure 2**a–e. The obtained yarns are nearly parallelly aligned and have a special axis along the drawing direction. In addition, the yarns are found to be elastic and pliable and can be freely manipulated and molded to any desired shape. The CNT yarns displayed excellent electrical conductivity of 300 S cm^{-1} and robust mechanical properties of 575 MPa g cm^{-3} at room temperature, considering the highly ordered macroscopic structures of the 1D nanomaterials. CNTs with 1D macroscopic morphology can also be created from aerogels that are prepared in hot regions of a reaction chamber through the floating-catalyst chemical vapor deposition (CVD) method,[44] and flexible ropes with a diameter of ≈1.5 mm and length of ≈3000 mm can be directly obtained by twisting CNT socks. CNT ropes display homogeneous and compact structures after passing through a drawing die, as shown in Figure 2f. Moreover, the formed ropes can be easily manipulated without any damage, such as bending, folding, twisting, or tailoring (Figure 2g). The formed ropes can also be twisted or untied easily without any interfiber adhesion, indicating their high strength and excellent flexibility. The surface structure of the prepared rope consists of long CNT bundles,

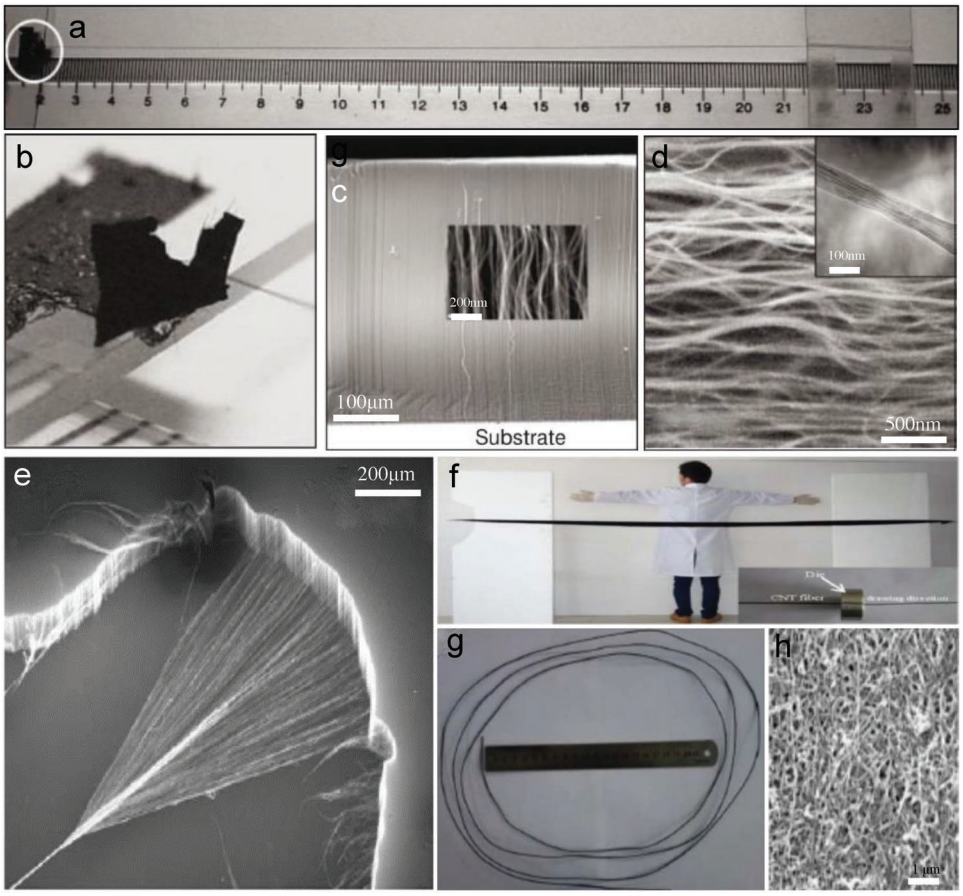

Figure 2. a) A CNT yarn being continuously pulled out from a freestanding CNT array, which is shown enlarged in (b) (roughly × 8 magnification). c) Scanning electron microscopy (SEM) images of a CNT array grown on a silicon substrate, showing the superalignment of CNTs. d) SEM image of the yarn in (a); inset, transmission electron microscopy (TEM) image of a single thread of the yarn. a–d) Reproduced with permission.[42] Copyright 2002, Nature Publishing Group. e) SEM image of a CNT yarn in the process of being simultaneously drawn and twisted during spinning from a nanotube forest. Reproduced with permission.[43] Copyright 2004, The American Association for the Advancement of Science. f,g) Typical images of CNT long sock (f), and rope (g); the inset shows the drawing process. h) SEM images of the rope. f–h) Reproduced with permission.[44] Copyright 2017, AIP Publishing.

and the bundles form an interconnected network (Figure 2h). The network may provide pathways for movement of mobile charges, showing excellent electrical and thermal conductivities, which are essential to achieve a high efficiency of electron conversion from the active materials to the current collectors.

Film-like CNTs are a relatively new form of macroscopic CNTs, with large 2D lateral surface areas; these film-like CNTs have been explored through solution-deposition methods, such as vacuum filtration,[45] solution spraying,[46] and deposition of dispersions.[47] The main advantage of these methods is their capability for directly yielding thin films at room temperature using formed CNTs by bulk preparation procedures. These techniques are limited to destructable nanotubes, which hampers the electrical properties. The films can also be directly extracted from superaligned CNT arrays.[48] The obtained films can be tailored into many shapes and mounted on various insulating surfaces shown in **Figure 3**a,b. However, the challenges include thickening these films, generating additional area, and enabling mass production.[49] Flexible CNT films (Figure 3c,d) can also be prepared directly through the floating-catalyst CVD method at the high-temperature zone of the chamber with robustness and high conductivity.[50] The firm bonding between the bundles of directly grown films results in an improved conductivity and strength. However, the area of the obtained films (Figure 3e–g) is limited by the diameter of the reaction chamber.[51] CNTs grown through the CVD, which can self-assemble into aerogel-like socks, have also been reported.[52] Large-area CNT films with high shape conformability and homogeneity can be fabricated in batches by controlling the interface between the CNT socks and substrates.[53] The sheet electrical resistances are stable and remain unchanged after folding, thereby confirming that the electronic properties of the films are insensitive to folding.

The production of macroscopically engineered structures based on assembled CNTs with controlled orientation and configuration is an important step toward practical applications. Sponge-like bulks with 3D framework have been demonstrated, as shown in **Figure 4**a–d; these bulks are composed of self-assembled, interconnected CNT skeletons with a density that is close to that of light aerogels, a porosity of >99%, high flexibility, and robustness.[23] CNT sponges can also be deformed to any shape elastically and compressed to large strains repeatedly

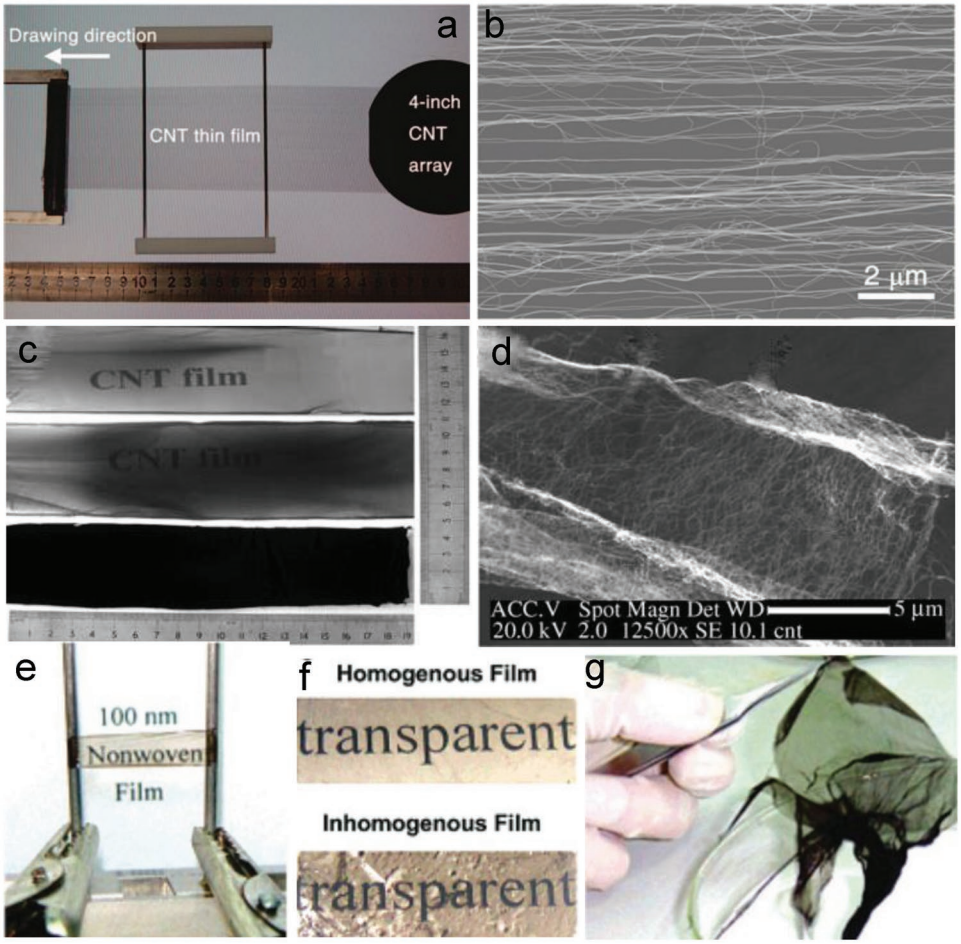

Figure 3. a) A CNT thin film was pulled from a superaligned CNT array grown on a 4 in. silicon wafer and put on two electrodes of a frame to make a loudspeaker. b) SEM image of the CNT thin film showing that the CNTs are aligned in the drawing direction. a,b) Reproduced with permission.[48] Copyright 2008, American Chemical Society. c) Optical image showing the different CNT films with varied thicknesses. d) SEM image of the film edge pulled out of the film. c,d) Reproduced with permission.[50] Copyright 2006, Wiley-VCH. e–g) Photographs of an as-grown 250 nm thick film (e), a transparent 100 nm-thick film freely stands between metallic pillars (f), and 150 nm-thick homogenous and imhomogeneous film (g). e–g) Reproduced with permission.[51] Copyright 2007, American Chemical Society.

in air or liquid without collapse (Figure 4e–h). The structural integrity under large deformations is due to the highly interconnected CNTs in a 3D isotropic configuration, which could prevent sliding between CNTs along any direction. The CNT sponges can be prepared through the CVD method and then collected at the quartz substrate in the reaction zone.

2.2. Graphene with Different Macroscopic Morphologies

Graphene is considered as an ideal material for energy devices[54–56] given its unique single-atomic-layer structure with high electrical conductivity, mechanical properties, and chemical stability. The mechanical exfoliation of graphite with Scotch tape was first used for this purpose and led to the discovery of graphene.[57] This method can produce high-quality graphene sheets with small sizes and low yield for fundamental research. However, it cannot be used to produce large amounts of graphene for energy applications. To further explore graphene in practical applications, versatile and reliable synthetic routes for single- or few-layer graphene sheets have been developed, ranging from CVD,[58,59] to chemical oxidation–reduction of graphite,[60,61] to ball-milling mechanical exfoliation.[62,63] Graphene production through CVD directly is a promising technique for producing graphene sheets with large areas and few defects. The critical step of the CVD method is transferring the graphene from the metal substrate to the desired substrate without degrading the quality of the graphene. However, the CVD method will result in residual poly(methyl methacrylate) (PMMA) on the graphene surface during transfer. Therefore, graphene prepared by CVD methods possesses a perfect structure with high carrier mobility, which could promote the conductivity of the electrode, but the yield is limited. By contrast, oxidative exfoliation of natural graphite to graphene oxide (GO), followed by GO reduction to obtain reduced GO (rGO), produces many defects and leads to nonideal properties, but the low-cost rGO with functional groups can achieve better binding with active materials, although the defects in rGO reduce electron conductivity and cause irreversible capacity during cycling. Different preparation methods actually lead to different

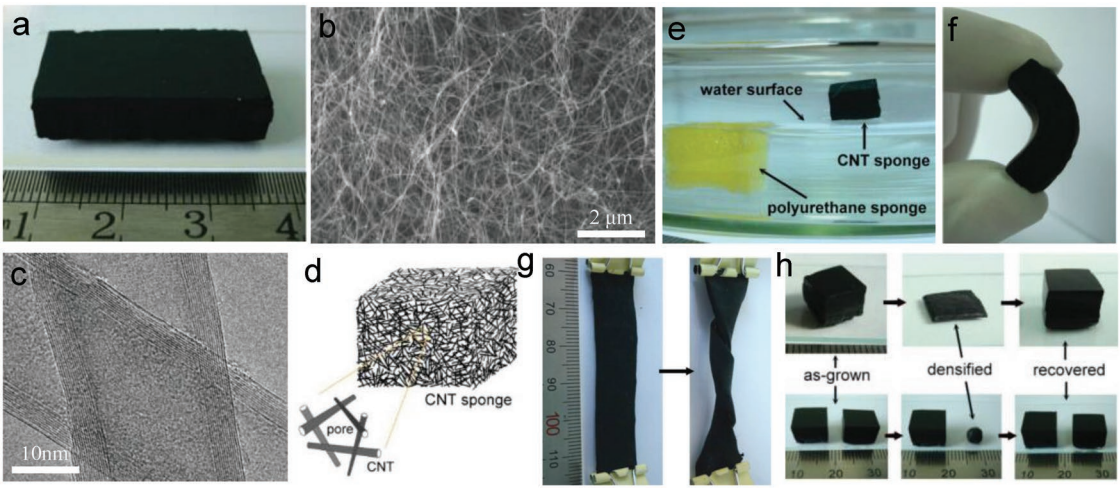

Figure 4. a) A monolithic sponge with a size of 4 cm × 3 cm × 0.8 cm and a bulk density of 7.5 mg cm^{-3}. b) Cross-sectional SEM image of the sponge showing a porous morphology and overlapped CNTs. c) TEM image of large-cavity, thin-walled CNTs. d) Illustration of the sponge consisting of CNT piles as the skeleton and open pores. e) Picture of a CNT and a polymeric sponge placed in a water bath. f) A CNT sponge bent to an arch-shape at a large-angle by the finger tips. g) A sponge twisted by three round turns at the ends without breaking. h) Densification of two cubic-shaped sponges into small pellets and full recovery to original structure upon ethanol absorption. a–h) Reproduced with permission.[23] Copyright 2010, Wiley-VCH.

materials with distinguished properties. Large-scale preparation of high-quality graphene and building uniform macroscopic structures such as graphene fibers (1D), graphene paper (2D), graphene foam (3D), or graphene ink are critical steps to enable its practical applications.

2D graphene films, i.e., graphene papers, are one of the most reported materials for flexible batteries. They can be prepared by the deposition of multilayer CVD graphene sheets in copper substrates directly.[64] The obtained 2D graphene films exhibit excellent physicochemical properties, but the tedious transfer process limits their application. Therefore, a cost- and time-saving roll-to-roll method was developed to address the above-mentioned problems.[65] In this case, the graphene on a flexible copper foil was attached to a thermal release tape by applying a weak pressure (≈0.2 MPa) between two rollers, as shown in **Figure 5**a,b. The graphene film on the tape was transferred on the surfaces of any flexible substrate after etching the copper foil, as shown in Figure 5c–e. This technique is scalable; a 30 in. multilayer graphene film was successfully transferred to a poly(ethylene terephthalate) (PET) roll for fabricating touch-screen panels. Graphene paper can also be prepared by vacuum filtration, coating, and dipping from the GO precursors[26] (Figure 5f–i). The structure and thickness of the prepared paper can be easily controlled. However, graphene sheets are easily stacked and aggregated. A layer-by-layer sequential assembly of positively and negatively charged rGO sheets based on dip coating has been developed to avoid the aggregation of graphene sheets.[66] The functional groups can enlarge the inter-sheet spacing and strengthen the interaction force.

In addition to graphene paper, 1D graphene fibers/yarns also have outstanding properties, such as high conductivity, light weight, extensive mechanical strength, and considerable specific surface areas. Moreover, graphene fibers/yarns can be fastened in tight knots without any breakage or can be integrated into conductive patterned textiles with other threads. Similar to carbon fibers and CNT yarns, graphene fibers can be fabricated by wet-spinning of the GO dispersion followed by chemical reduction, as shown in **Figure 6**a–j.[67] Hydrothermal reduction of a GO suspension sealed in a long and thin tube could produce conductive rGO fibers to shorten the process (Figure 6i–p).[68] Moreover, 1 mL of GO suspension (8 mg mL^{-1}) can generate rGO fibers that are longer than 6 m (≈35 μm in diameter) by using a glass pipeline of 0.4 mm inner diameter; the rGO fibers exhibit a density that is less than 1/7 of that of conventional carbon fibers. Large-scale preparation of graphene fibers can be conducted by maximizing the pipelines and ovens, and continuous production of graphene fibers by setting up a thermal-flow circulatory pipeline system is in progress. The obtained graphene fibers can be shaped with the required specific geometry and exhibit excellent mechanical properties. The robust but low-weight graphene fibers with appropriate functionalization and controllable shaping and stitchability can be integrated into flexible and hierarchically engineered structures for various specific applications, such as smart clothing and electronic textiles.

Poor bonding and low interfacial strength are found between the active materials and 1D fibers/2D films when they are applied in energy devices. Thus, 3D graphene foams have been developed to improve the loading and adhesion stresses. 3D graphene frameworks demonstrate unique properties, such as high porosity, huge specific surface area, light weight, and excellent electrical conductivity. Typical 3D graphene materials include foams,[69,70] sponges,[71,72] hydrogels,[73,74] and aerogels.[75,76] 3D graphene materials are typically prepared through self-assembly of graphene sheets from GO precursors, as shown in **Figure 7**a–f.[77] The self-assembly behavior of the GO sheets in aqueous media is mainly controlled by the balance between interplanar van der Waals force and electronic repulsion of GO sheets. The properties of the 3D graphene are determined by the size and concentration of the GO precursors. Many joint molecules have been introduced, as shown in Figure 7g–j, to strengthen the interaction force of

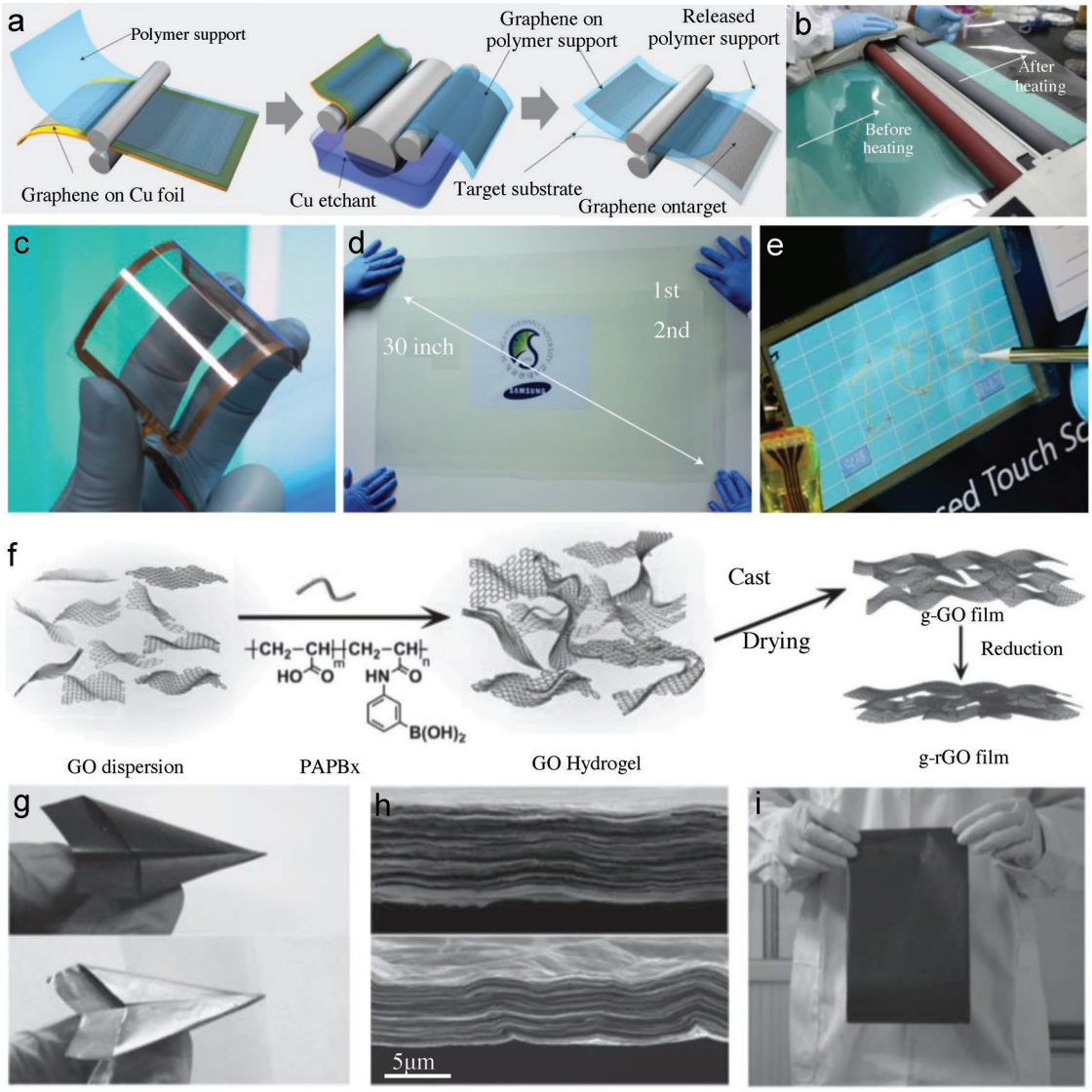

Figure 5. a) Schematic process of roll-based production of graphene films grown on a copper foil. b) Roll-to-roll transfer of graphene films from a thermal-release tape to a PET film. c) A transparent ultralarge-area graphene film transferred on a 35 in. PET sheet. d) An assembled graphene/PET touch panel showing outstanding flexibility. e) A graphene-based touch-screen panel connected to a computer with control software, a–e) Reproduced with permission.[65] Copyright 2010, Nature Publishing Group. f) Mass production of g-GO and g-rGO films by a cost-effective gel-film transformation method. g) Photographs of g-GO (top) and g-rGO (bottom) films, showing their flexibility. h) SEM images of the fractured cross sections of g-GO (top) and g-rGO (bottom) films, exhibiting their laminated structures. i) Photograph of a large-area g-GO film. f–i) Reproduced with permission[26] Copyright 2014, Wiley-VCH.

the 3D graphene.[27,78] An ultralight and highly elastic graphene aerogel with an interpenetrating binary network is prepared. The composite aerogel shows favorable mechanical strength, high electrical conductivity, and a higher specific capacitance than compact graphene films. The porosity of the foam can also enhance the accessibility of lithium ions and electrolytes, thereby providing a higher performance than graphene films that were fabricated through a flow-directed assembly method.

Besides the above methods, another important trend in wearable electronics is to deposit conductive ink onto a flexible substrate to form a flexible conductive electrode. The key issue in the method is to develop conductive inks with good dispersion. However, the dispersion of high concentrations of graphene in solution is still a great technical challenge due to the strong stacking interactions between the planar graphene sheets.[79]

2.3. CNT–Graphene Composites with Different Macroscopic Morphologies

1D CNTs and 2D single-atomic-layer graphene demonstrate superior electrical, thermal, and mechanical properties. However, these nanomaterials exhibit poor out-of-plane properties given the weak van der Waals interactions in the transverse direction between the graphitic layers.[80,81] To ensure that the CNT–graphene structures display efficient electrical

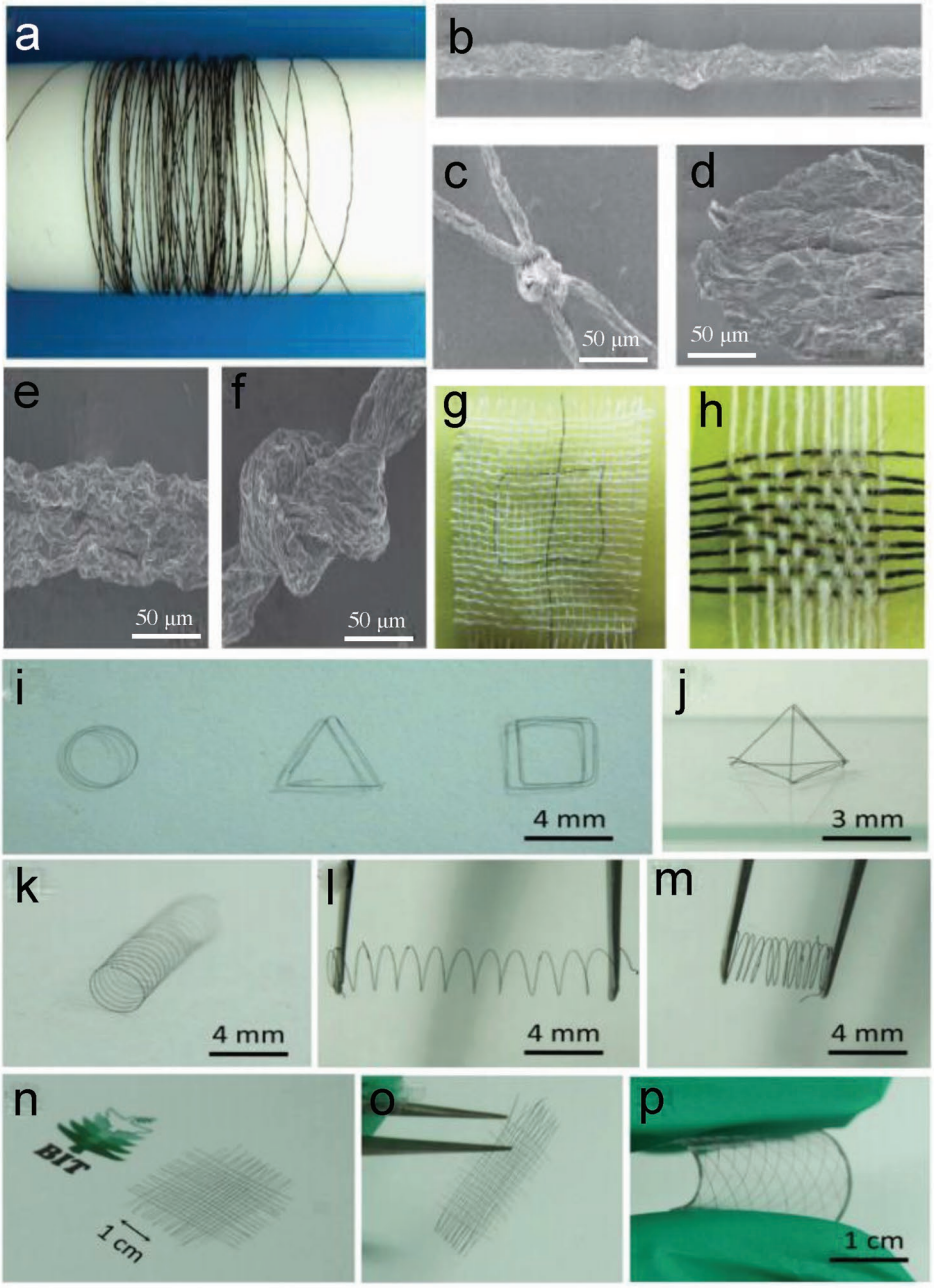

Figure 6. a) Four-meter-long GO fiber wound on a Teflon drum (diameter, 2 cm). b,c) SEM image of the fiber (b), and its typical tightened knots (c). d) The fracture morphology of GO fiber after tensile tests. e,f) The surface winkled morphology (e); and the tightened knot of graphene fiber (f). g) A Chinese character ("中," Zhong) pattern-knitted in the cotton network (white) using two graphene fibers (black). h) A mat of graphene fibers (horizontal) woven together with cotton threads (vertical). Scale bars: b–f) 50 μm and g,h) 2 mm. a–h) Reproduced with permission.[67] Copyright 2012, Wiley-VCH. i,j) Shaping and weaving of graphene fibers and the handmade planar (i) and 3D (j) geometric structures of graphene fibers. k–m) The spring made from graphene fiber in free, stretched, and compressed states, respectively. n,o) Photographs of the hand-knitted textile of graphene fibers. p) Photograph of graphene fiber network embedded in a PDMS matrix shaping and weaving of graphene fibers. i–p) Reproduced with permission.[68] Copyright 2012, Wiley-VCH.

and thermal transport characteristics in all directions, several groups have demonstrated the use of CNT–graphene composite fibers to create a seamless pure C—C nodal junction between the constituent CNT and graphene. Dai and co-workers[82] developed a one-step CVD method without an additional metal nanoparticle catalyst to directly grow hollow fibers made of CNTs constrained by cylindrical graphene layers. The composite fibers show a large surface area of 526.91 m^2 g^{-1} and minimized interfacial electrical/thermal resistances. Peng and co-workers[83] prepared CNT–graphene composite fibers with graphene sheets that were incorporated among neighboring CNTs to serve as effective bridges to

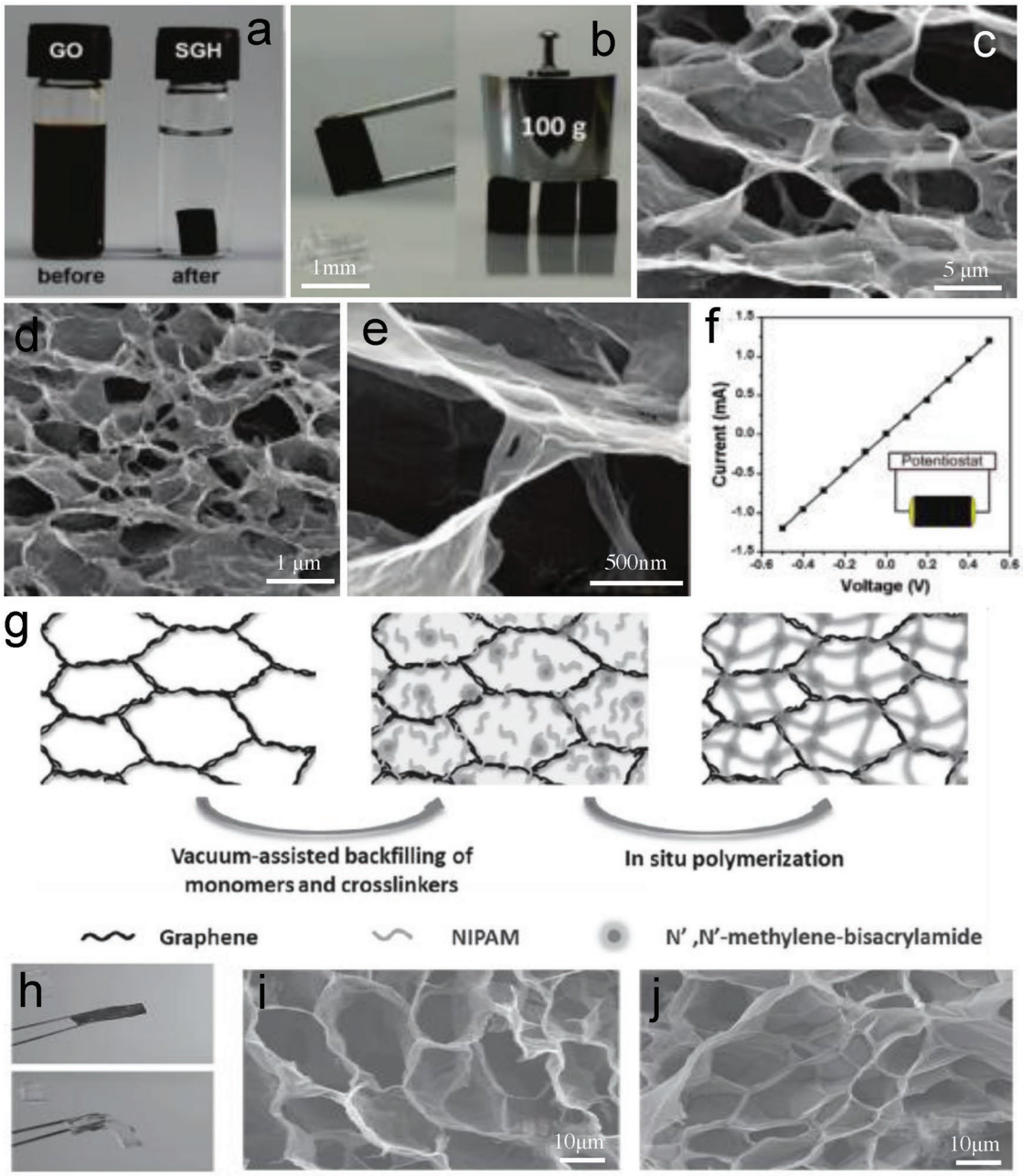

Figure 7. a) Photographs of a 2 mg mL^{-1} homogeneous GO aqueous dispersion before and after hydrothermal reduction. b) Photographs of a strong SGH allowing easy handling and supporting weight. c–e) SEM images with different magnifications of the SGH interior microstructures. f) Room temperature *I–V* curve of the SGH; the inset shows the two-probe method for the conductivity measurements. a–f) Reproduced with permission.[77] Copyright 2010, American Chemical Society. g) Synthesis scheme for preparation of GABN hydrogels. h) Photographs of GABN and PNIPAM hydrogels. i,j) SEM images of graphene aerogel (i) and freeze-dried GABN (j). g–j) Reproduced with permission.[78] Copyright 2014, Wiley-VCH.

improve the charge transport. High electrical conductivity and electrocatalytic activity of the obtained novel fibers have been simultaneously achieved.

Bendable CNT–graphene films have also been developed. Xue and co-workers[84] reported CNT–graphene films through an extended filtration-assisted method. The graphene nanosheets maintain the integrity of the film and provide flexibility. CNTs can also serve as hard spacers in the hybrid structure. Such asymmetric system is expected to possess the advantages of capacitors and batteries. CNT–graphene films can also be woven from hybrid fibers.[85] The hybrid fibers are produced with increased toughness, high surface area, and conductivity by solution-spinning of graphene and CNT. Then, the fibers are woven into textile electrodes for the construction of flexible energy-storage devices with high tolerance to repeated bending cycles. CNT–graphene hybrid films can also be prepared based on the self-assembly of CNTs and GO. A simple drop-casting method of mixing the components into a slurry is

performed, and the substrate is coated to produce composite films.[86] The hybrid films provide promising applications for novel electrochemical devices. A 2D auxetic cellular honeycomb structure of rGO/CNT was also obtained by compressing a vertically aligned array of rGO/CNT networks.[87] The reentrant structures showed enhanced strain tolerance and areal/volumetric capacitances to the electrode and promoted the diffusion of electrolyte ions by behaving as ionic highways.

Several strategies to fabricate CNT–graphene 3D architectures have also been applied, in which GO–CNT aqueous mixtures can be directly cryodesiccated to form composite aerogels with light weight and tunable densities.[88] The macroscopically assembled and all-carbon aerogels provide integrated properties of low density, temperature-invariant high-recyclable compressibility, and elastic responsive conductivity. Stacked nanoporous graphene layers pillared with CNTs were prepared to accommodate the CNTs within the graphene to increase the accessible surface area and create efficient ion-diffusion pathways. The advantages of the 3D porous structure are its medium mass density and high electrical conductivity; these advantages are important for obtaining high volumetric and gravimetric densities. In a word, 3D architecture materials composed of CNT and graphene with porous structures and high conductivity provide diversified candidates toward constructing electrodes on flexible energy storage systems.[89]

3. Application in Flexible Batteries

In recent years, carbon nanomaterials, including CNTs and graphene, have been widely investigated as current collectors or freestanding active materials for different batteries given their low contact resistance, robust adhesion, and mechanical durability.[90–93] A crucial key to this end is to develop flexible electrodes with a fiber-shape or paper-like morphology. The 1D electrode can accommodate various deformations in the length direction and can be woven into textiles to satisfy the various shapes of our bodies.[94–96] The 2D electrode can provide flexible, thin, lightweight features, and high mass loading of active materials and possesses a significant potential to be fully integrated with flexible electronics. Different kinds of flexible batteries[97] with a 1D or 2D structure have developed rapidly since the flexible LIB was reported in 2010.[98] The energy density of these flexible batteries was also reported in recent studies.[99]

3.1. 1D Flexible Batteries Based on Carbon Nanomaterials

The flexibility of 1D batteries means that designers are free from conventional constraints, because these batteries can be placed anywhere in any shape. Moreover, the batteries can be worn on the wrist, neck, or any other part of the body to realize the practical application of wearable electronics, rather than mounting these batteries inside electronic devices.[100] The development of 1D electrodes is the core for batteries with fiber-shaped morphology. In addition, other components of 1D batteries should be assembled with fiber-shaped structures.[101] Recently, the main efforts have been focused on preparing carbon nanomaterials or integrating active materials that can effectively mix or support active materials as freestanding electrodes with fiber morphology.[102] Several types of batteries have been developed, including LIBs, lithium–sulfur batteries, lithium–air batteries, zinc–air batteries, aluminum–air batteries, silicon–oxygen batteries, sodium-ion batteries, and silver–zinc batteries.

3.1.1. 1D Flexible LIBs

After ITN researchers showed a proof of concept[103] that it is possible to layer battery materials on curved fibers, LG Chem, Ltd. achieved a 1D cable LIB based on hollow multihelix electrodes in 2012 to realize the 1D concept.[104] The fabrication of cable batteries can be separated into two steps as follows. First, copper wire is electrodeposited, and a hollow-helix nickel–tin alloy anode is fabricated. Secondly, a PET separator and the cathode made of aluminum-wire coated $LiCoO_2$ (LCO) are looped around the anode and assembled for full batteries. It was suggested that the obtained batteries can be connected or woven in parallel or in series, thereby resulting in various shapes. However, the active-material mass loading, specific capacity, and energy density of the battery are not high. In addition, the flexibility of the battery should be improved further for practical applications.

In 2013, Peng and co-workers developed a 1D battery by twisting aligned CNT fibers and lithium-metal wires, which functioned as positive and negative electrodes, respectively.[105–107] MnO_2 nanoparticles were uniformly deposited in CNT fibers in an aqueous solution. The flexible battery showed a high specific capacity of 94.37 mAh cm^{-3} or 174.4 mAh g^{-1} based on active material. The charge/discharge energy densities of the 1D battery were 92.84 and 35.74 mWh cm^{-3}. To improve the specific capacity and cyclic stability of flexible battery, Si was evaporated on CNT sheets from aligned CNTs by an electron beam and then twisted to prepare CNT/Si composite fibers.[108] The composite fiber and lithium metal wire were connected to copper wires to assemble the LIB. The battery, with flexibility, displays a higher specific capacity (based on the mass of Si) of 1970 mAh g^{-1} at the 50th cycle than that of 1648 mAh g^{-1} at the 30th cycle in a pure Si anode. Furthermore, the failure behavior of a 1D battery based on CNTs has also been investigated.[109] The results indicated that the loss of electrical contact between the current collector/conductive network and the active material is the dominant failure mechanism. Specifically, the interphase contact between the active materials and the CNTs unfastens gradually, resulting in a decreased capacity. The lithium-metal wire was replaced by lithium manganite (LMO) for a 1D battery, considering the safety, working voltage, and structural stability of the battery.[110] The LMO was incorporated into an aligned CNT fiber as the cathode, and the above CNT/Si was used as the anode. The obtained coaxial fiber full battery showed a linear capacity density of 0.22 mAh cm^{-1} and linear energy density of 0.75 mWh cm^{-1} based on the cathode. The fiber-shaped battery could also be woven into a flexible energy-storage textile with an areal energy density of 4.5 mWh cm^{-2}. The dendritic lithium on the anode results in a short circuit and combustion. The anode material of $Li_4Ti_5O_{12}$ (LTO) on CNTs with a high lithiation potential was used to prevent the problem of the dendritic lithium, and LMO was used as the cathode for fiber-shaped batteries.[111] The battery exhibited a high energy density

of 27 Wh kg^{-1} or 17.7 mWh cm^{-3} based on the overall volume of the electrode materials of the full battery. The battery could also sustain thousands of repeated deformations with only a minimal decrease in capacity, as shown in **Figure 8**. In addition, a battery based on CNTs could be integrated with a photoelectric conversion into a flexible fiber.[112] The 1D integrated energy device exhibited a core–sheath structure with the photoelectric conversion at the sheath and the LIB at the core. The 1D device provided a high energy density of 22 Wh kg^{-1} based on active material and an output voltage of 2.6 V to power various electronic devices. 1D aqueous LIBs were created by using a polyimide/CNT hybrid fiber as the anode, an LMO/CNT fiber as the cathode, and lithium sulfate aqueous solution as the electrolyte, considering the low power density of the 1D battery based on carbon nanomaterials and flammable and toxic organic electrolytes.[113] The battery with flexibility output a power density of 10217.74 W kg^{-1} based on the total mass of the battery, and, at the same time, the safety issue generated by traditional electrolytes was resolved. Wang et al.[114] developed a 3D fabrication technology to fabricate 1D LIBs toward flexible energy storage. CNTs were used as a conductive additive to facilitate the transport of electrons. The obtained flexible battery exhibited a high discharge specific capacity of 110 mAh g^{-1} at 50 mA g^{-1} based on active material. The abovementioned fiber electrodes had extremely low loading of active materials and weak adhesion between the active materials and the current collector. A molecular hybridization of rGO with titanium sheets for 1D batteries was reported.[115] This study eliminated the linear substrate backbone and directly used active materials to build 1D LIBs. The material displayed a plastic deformation, which was due to the displacements of the rGO sheets in the stacking structure. In 2018, our group invented a lithium-ion 1D battery that is insensitive to deformation, due to its use of CNT woven macrofilms as the charge collectors.[116] The prototype and flexibility of the battery can be seen clearly in **Figure 9**. An ultrahigh tap density of 10 mg cm^{-2} of the electrodes could be obtained, which led to an extremely high energy density of 215 mWh cm^{-3} based on the whole volume of the battery. In addition, the battery displayed a more stable rate performance and lower internal resistance than conventional LIBs using

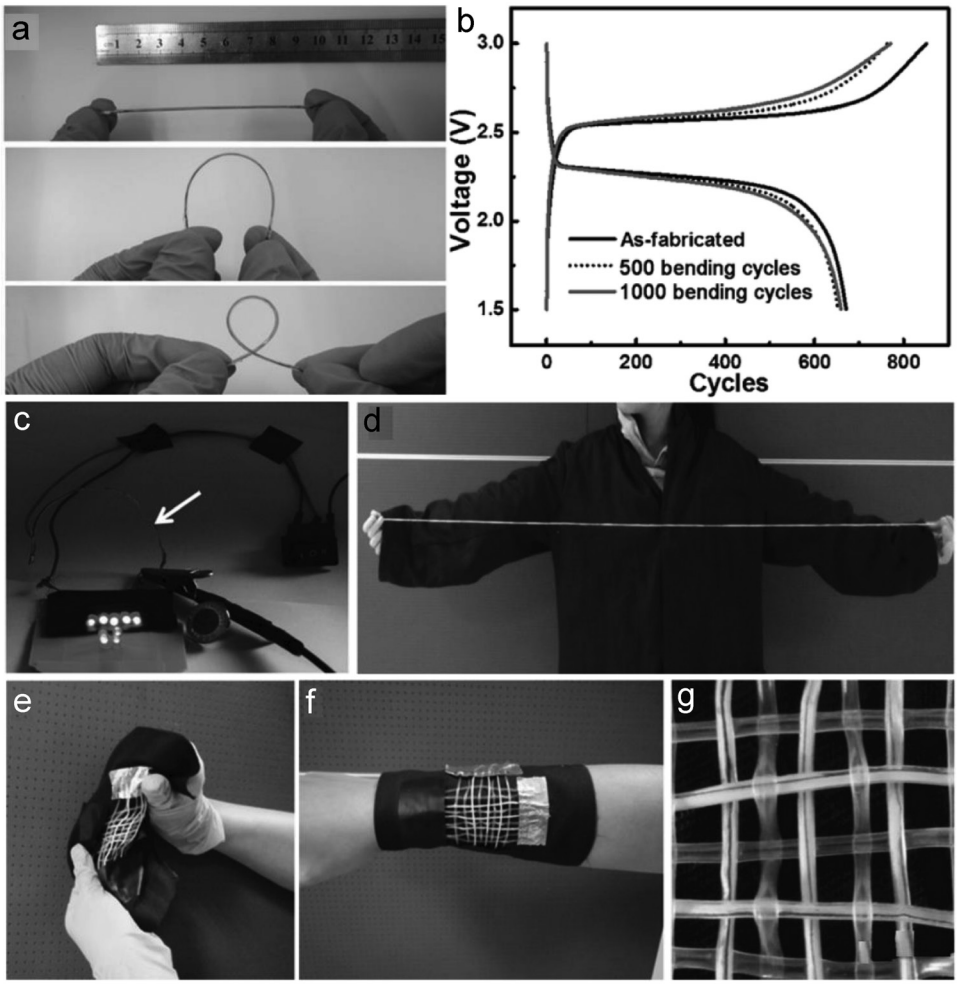

Figure 8. a) Photographs of a fiber-shaped battery being deformed into different shapes. b) Galvanostatic charge and discharge curves before and after bending for 500 and 1000 cycles at 0.05 mA. c) Nine light-emitting diodes being powered by a fiber-shaped battery with a length of 10 cm. d) A long fiber-shaped lithium-ion battery with a length of 200 cm. e–g) Fiber-shaped batteries woven into flexible textiles. a–g) Reproduced with permission.[111] Copyright 2014, Wiley-VCH.

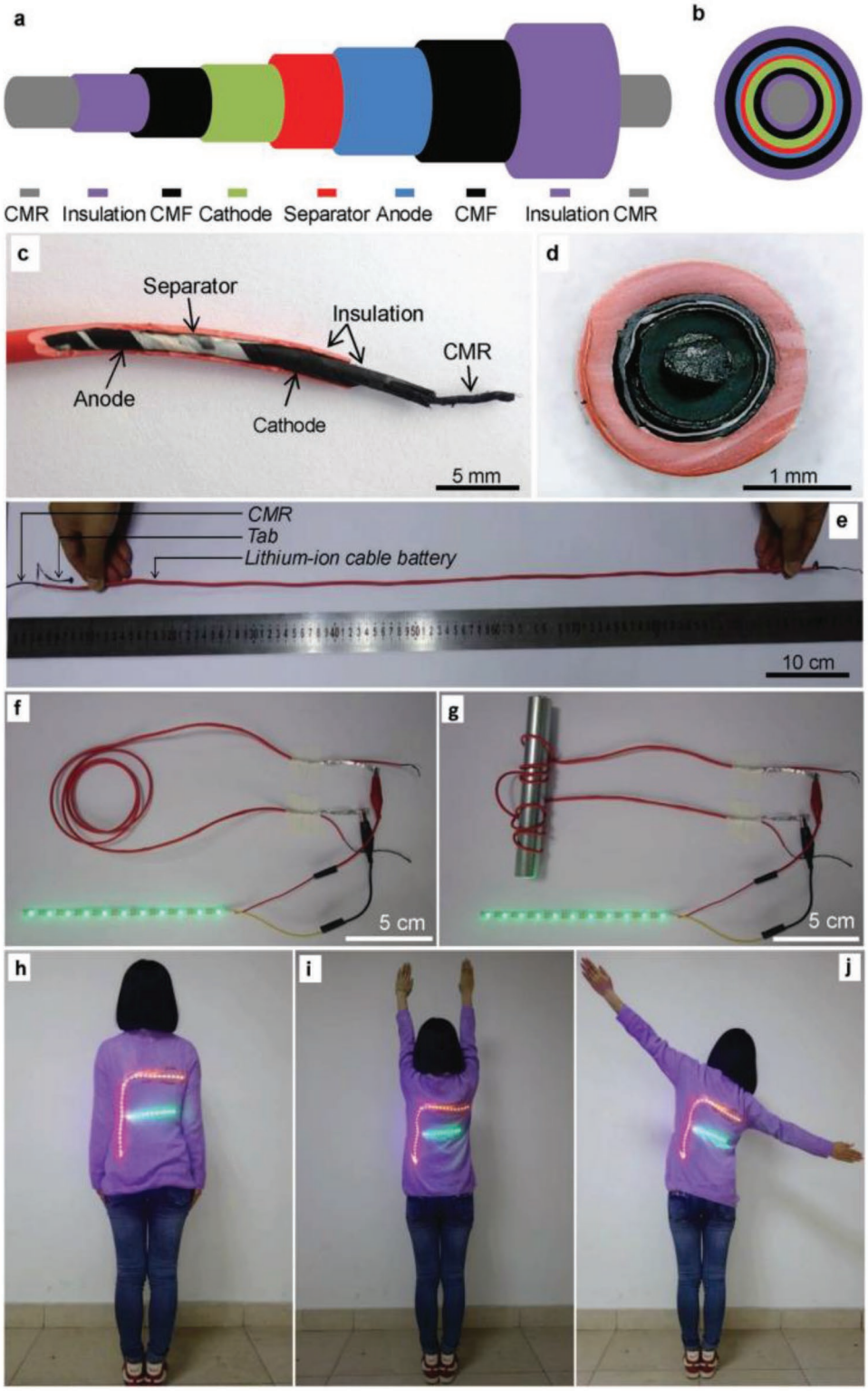

Figure 9. Schematic diagram and prototype of the lithium-ion 1D battery: a) side view schematic, b) cross-sectional schematic, and c) photograph of the battery in side view. d,e) Cross-section (d) and prototype of the battery including CNT macro-rope (e). f,g) The battery in the free state (f) and twisted on a rod (g). h–j) LED lights, and the wearable lithium-ion 1D battery on the body during exercises. Reproduced with permission.[116] Copyright 2018, Wiley-VCH.

metal charge collectors. Moreover, it demonstrated excellent convenience for connecting electronics, as we applied a new strategy, in which both electrodes could be integrated into one end by a CNT macro-rope.

According to the above discussions, both CNTs and rGO can be used for the preparation of 1D flexible LIBs. The main issue is about the efficiency of electron conversion from the active materials to the current collectors. Highly conductive pathways for the movement of mobile charge can be provided by the CNT networks. Limited to the aforementioned technologies, the tap densities of the active materials on the present flexible and thin carbon nanomaterials are not high, resulting in low energy densities. In addition, both the gravimetric and volumetric energy density will be reduced further if metals are used as charge collectors due to the increase in both the weight and volume of the packages. Moreover, the metals used in batteries are not suitable when worn on the body. Therefore, the energy density of the current batteries should be developed further for practical applications.

3.1.2. 1D Flexible Lithium–Sulfur Batteries

Other types of batteries based on carbon nanomaterials have been investigated in terms of high specific capacity and energy density given the theoretical limitation in storing electrode materials. Lithium–sulfur batteries with a specific capacity of 1675 mAh g^{-1} and energy density of 2600 Wh kg^{-1} are considered to be a promising battery system.[2] Peng and co-workers[117] developed a 1D lithium–sulfur battery using CNT as the current collector and GO layers as physical barriers. The specific capacity of the as-prepared battery was 800 mAh g^{-1} based on active material at a current rate of 0.1 C, and the open-circuit voltage of the battery was 3.2 V. Moreover, Liu et al.[118] studied lithium–sulfur batteries using rGO as a support to load sulfur. Then, the rGO/sulfur composites were self-assembled on the surface and interfilament spacing of a stainless-steel fiber to form fibrous cathodes, as shown in **Figure 10**a. The fibrous cathode delivered a substantial capacity of 702.3 mA g^{-1} based on active material at 0.1 C and excellent flexibility, as shown in Figure 10b–f. Meanwhile, a 1D lithium–sulfur battery with flexibility based on CNT–graphene has also been reported.[119] In this study, rGO/CNTs and binder-free sulfur composites were prepared as spinning dopes, in which fibers could be fabricated by the wet-spinning approach. The result demonstrated a competitive areal energy density with a sulfur loading of 2 mg cm^{-2}. The corresponding volumetric capacity and energy density of the battery were 440 mAh L^{-1} and 917 Wh L^{-1} based on active material, respectively. Similar to the above flexible LIBs, 1D lithium–sulfur batteries can be fabricated based on CNTs and graphene. They are used as a support for loading sulfur. Therefore, the electronic conductivity of the carbon nanomaterials is the main reason for improving the performance of the batteries. Another main issue is the mass loading of sulfur that can be deposited on the CNTs or graphene, the energy density of the batteries will be increased with an increase in the mass loading of the active materials.

3.1.3. Other 1D Types of Flexible Batteries

The reversible reaction of lithium and oxygen exhibits a high theoretical specific energy density of 3500 Wh kg^{-1}. Therefore, lithium–air batteries are proposed as a next-generation energy-storage system.[120] However, this type of battery experiences parasitic reactions and low recyclability in ambient air. The lithium–air battery with its high electrochemical performance and flexibility has been investigated with aligned CNT sheets wrapped around as the air electrode and a gel polymer as an all-solid electrolyte.[121] The battery exhibited a discharge capacity of 12 470 mAh g^{-1} based on the weight of the CNT electrode at a current density of 1400 mA g^{-1}, and could effectively work for 100 cycles in air. In addition, the battery was demonstrated to be able to power electronics at various bent and twisted conditions. Zinc–air batteries also show broad perspectives for practical applications considering their low cost, environmentally friendly characteristics, and theoretical energy density.[122] A rechargeable zinc–air battery with a fiber shape was fabricated based on an aligned and cross-stacked CNT sheet for the oxygen reduction reaction (ORR) and to load RuO_2-based catalyst for the oxygen evolution reaction (OER).[123] The energy and power densities of the battery were calculated as 6 Ah L^{-1} and 5.7 Wh L^{-1}, respectively, based on the volume of the battery. Furthermore, it was bent to 30°, 60°, 90°, 120°, and 150° without obvious damage to the structure. The fabricated Co/N/O-tridoped graphene was also used for assembling a zinc–air battery.[124] The intrinsic structural defects in nanocarbon with highly active sites and hierarchical porous scaffolds exhibit excellent ORR and OER bifunctional activities. An open-circuit voltage of 1.44 V was observed even under bending when the batteries were integrated into the rechargeable zinc–air battery. Aluminum–air batteries have also been investigated in terms of their high theoretical energy density. Aligned CNT sheets can provide a porous framework to effectively adsorb oxygen, which can be reduced to OH^- at the cathode, after using Ag nanoparticles as the catalyst loaded on the CNTs.[125] Thus, 1D aluminum–air batteries with a specific capacity of 935 mAh g^{-1} and energy density of 1168 Wh kg^{-1} based on the consumed aluminum anode can be fabricated. In addition, the batteries can be woven into textiles due to their flexibility. The Ag-coated CNT sheets act as both a gas-diffusion layer and a current collector, and no other conductive additive or binder is added to the electrode. CNTs can also be used for loading Si nanoparticles to produce Si/CNT hybrid fibers and serve as the cathode for silicon–air batteries.[126] The corrosion of the Si/CNT fiber by oxygen and water in air can be prevented by the electrolyte. The silicon–air battery shows an energy density of 512 Wh kg^{-1} (based on the total weight of the two electrodes) and can work after bending for 20 000 cycles. The extensive geological distribution of sodium resources is expected to make sodium-ion batteries cheaper and safer than LIBs. A sodium-ion battery with a fiber shape was made by assembling a sodium wire and a separator with a cotton textile coated with Prussian blue and a GO composite. The GO was demonstrated to be valuable in supporting the Prussian blue with strong adhesion. Such 1D sodium-ion batteries display a capacity of over 110 mAh g^{-1}, based on active material, and a long life of 1800 cycles.[127] The specific capacity of the battery remained almost unchanged as compared before and after bending to 30° and 60°, even after bending to 90°, demonstrating the high stability and flexibility of the sodium-ion battery. The electronic conductivity, mass loading, and oxygen

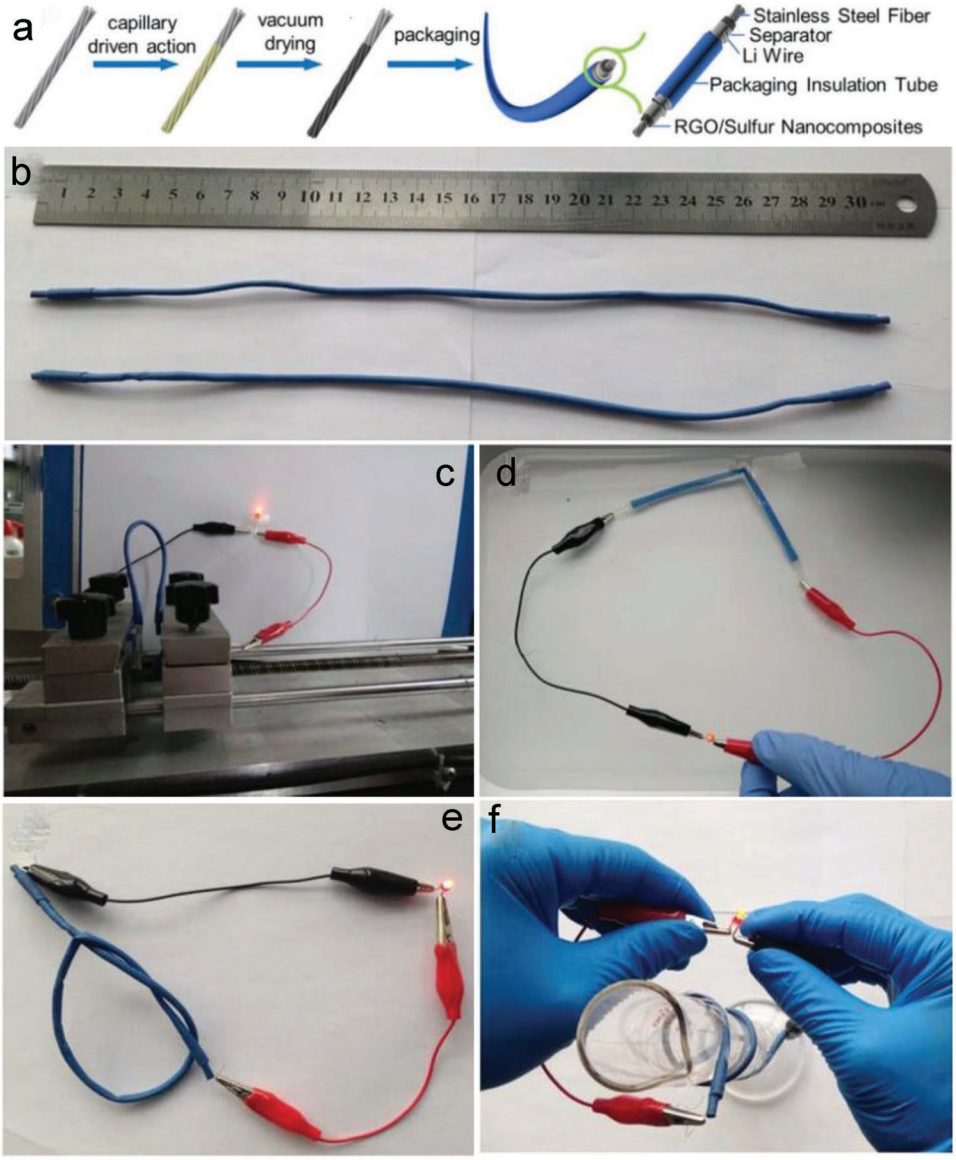

Figure 10. a) Scheme of synthesis of fiber-shaped lithium–sulfur electrode by the capillary action, and schematic and internal structure of the as-fabricated fiber-shaped lithium–sulfur battery. b) Optical image of the fiber-shaped lithium–sulfur battery with length of 30 cm. Demonstration of the flexibility of the as-fabricated fiber-shaped lithium–sulfur battery. c–f) Photographs displaying a red LED lit up by the fiber-shaped lithium–sulfur battery bent at 90° under water without waterproof measures (c), at nearly 180° deformation (d), and under knotting deformation (e) and twisting deformation (f). a–f) Reproduced with permission.[118] Copyright 2017, Elsevier.

permeation rate will determine the performance of metal–air batteries that are based on a support of CNTs and graphene. High electrocatalytic performance resulting from the CNTs and graphene would demonstrate better performance of the batteries. However, both the gravimetric and volumetric energy density of the batteries will be reduced if metals are used as the electrodes due to the increase in both the weight and volume of the packages. In addition, when metal is used as the electrode, they are neither thin nor flexible for wearable applications.

As previously discussed, carbon nanomaterials, such as CNTs, graphene, or their composites,[128] have been investigated by widely examining various kinds of batteries with fiber-shaped structure. In addition, the reported 1D batteries based on carbon nanomaterials show advantages, and can be integrated into textiles. Thus, these batteries can be woven into any shape and are practical for powering electronics. The high specific capacity and energy density of different types of batteries with fiber-shaped structures will play a significant role in wearable electronic devices with future carbon nanomaterial optimization and structure design improvements. The different parameters of the reported batteries with a fiber-shape are listed in **Table 1**. The results indicate the mass loading of the active materials, and the actual volume energy density of the obtained batteries should be improved further for practical applications.

Table 1. The performances of reported 1D flexible batteries.

Battery type	Voltage [V]	Specific capacity [mAh g^{-1}]	Active material mass loading [mg cm^{-2}]	Active material mass loading [mg cm^{-1}]	Battery diameter [mm]	Actual volume energy density[a] [mWh cm^{-3}]
LMO–CNT/LTO–CNT[111]	2.5	138	0.01	0.02	1	0.89
LMO–CNTs/PI–CNTs[113]	1.4	120	0.002	0.01	2	0.05
Titania/$LiMn_2O_4$ fiber battery[115]	3.5	168	–	0.12–0.19	1.5	4.0–6.3
LCO–Al/(Ni–Sn)–Cu[104]	1.7	1 mAh cm^{-1}	–	1.3	2.5	20.4
Li–S[117]	2.1	600	0.05	0.2	1	32.1
Li–S[118]	2.1	335	0.28	0.04	2	0.9
Li–S[119]	2.1	343	2	2	3	20.4
Li/O_2–SP–carbon textiles–nickel foam[120]	2.0	500	0.5	0.5	10	0.64
Li/O_2–Ag–CNT[121]	2.0	500	0.005	0.008	5	0.04
Zinc–air[122]	0.9	–	0.796	2.4	10	3.6
Zinc–air[123]	1	12 470	0.0014 *n*	0.05	3	5.7
Al–air[125]	1.65	935	0.07	0.01	3	0.22
LCO–CNT/LTO–CNT[116]	2.5–2.7	130	10	20	2	215

[a]Actual volume energy density = voltage × actual volume specific capacity.

3.2. 2D Flexible Batteries Based on Carbon Nanomaterials

2D batteries can provide a high flexibility and can be integrated into various wearable electronics. Thus, the different types of flexible batteries, including LIBs, lithium–sulfur batteries, lithium–air batteries, lithium–carbon-dioxide batteries, and aluminum-ion batteries, with this structure have been widely investigated. The key materials concerning this issue for wearable electronics are carbon nanomaterials, including CNTs and graphene.

3.2.1. 2D Flexible LIBs

LIBs are a common power supply given their high energy density, but the conventional rigid and heavy metal current collectors have prompted researchers to find a lighter replacement. Therefore, light CNTs with high electric conductivity have attracted considerable attention; the metal current collector could also be replaced to reduce the weight of the LIB significantly.[129] Subsequently, a flexible LIB using a flexible CNT film as the current collector has been explored.[98] The freestanding CNT thin film and active materials in the study were integrated into a paper through a lamination process, as shown in **Figure 11**a. The paper functioned as a mechanical substrate and a separator with low impedance. The rechargeable lithium-ion paper battery with 108 Wh kg^{-1} based on the total mass of the device was capable of bending down to less than 6 mm bending radius after packaging, as shown in Figure 11b. Due to LTO being used as the anode in the work, the working voltage could be improved by other technologies for practical applications. CNT films obtained from continuously aligned CNT arrays can be engineered into a roll-to-roll process and are feasible for commercial battery production. Therefore, aligned CNT films as the current collector and electrochemically active substrate for depositing Si[130] and graphite[131] active material have been investigated. The horizontal superaligned CNT films provide a high surface area and porous structure to facilitate the electrochemical kinetics between the Si and the electrolyte, and the specific capacity is maintained at approximately 1000 mAh g^{-1} based on active material with a current density of 800 mA g^{-1}; a stable cycle performance of the battery has also been observed. Flexible and freestanding graphite–CNT electrodes were easily produced, with structural integrity, excellent mechanical durability, and efficient electron transfer at the electrode/CNT interface because the graphite slurry was coated on top of the aligned CNT film. In addition, an outstanding cycling stability of 335 mAh g^{-1} based on the weight of the active graphite material at 0.1 C with capacity retention of 99.1% after 50 cycles could be obtained. Furthermore, the contact resistance was lower at the electrode/CNT interface than in the electrode/metal current collector. However, the thin thickness of films determined that the mass loading of active materials is not high, and therefore the energy density cannot be improved further. In addition, organic polymer packaging material and liquid electrolytes also should be explored for high flexibility and safety of the obtained batteries.

The art of paper folding has recently been applied to impart compactness and 3D morphologies on devices, and the required flexibility of the corresponding batteries should have the capability of being bent or folded. A major breakthrough in foldable LIBs was achieved by Cheng et al.[132] and Song et al.[133] at the Arizona State University. CNT ink was deposited on laboratory Kimwipes, which were used as the current collector. The use of the flexible Kimwipe tissues enabled the CNT ink electrode to be successfully folded in various patterns in an LIB. The results showed that the assembled full cell had a thinness of only 380 μm. The mechanical characteristics of the fully charged battery using 45° Miura folding were stable, as shown in **Figure 12**a,b. The output voltage under folding and unfolding remained steady at 2.65 V, especially on a linear deformability in terms of its completely compressed state. In

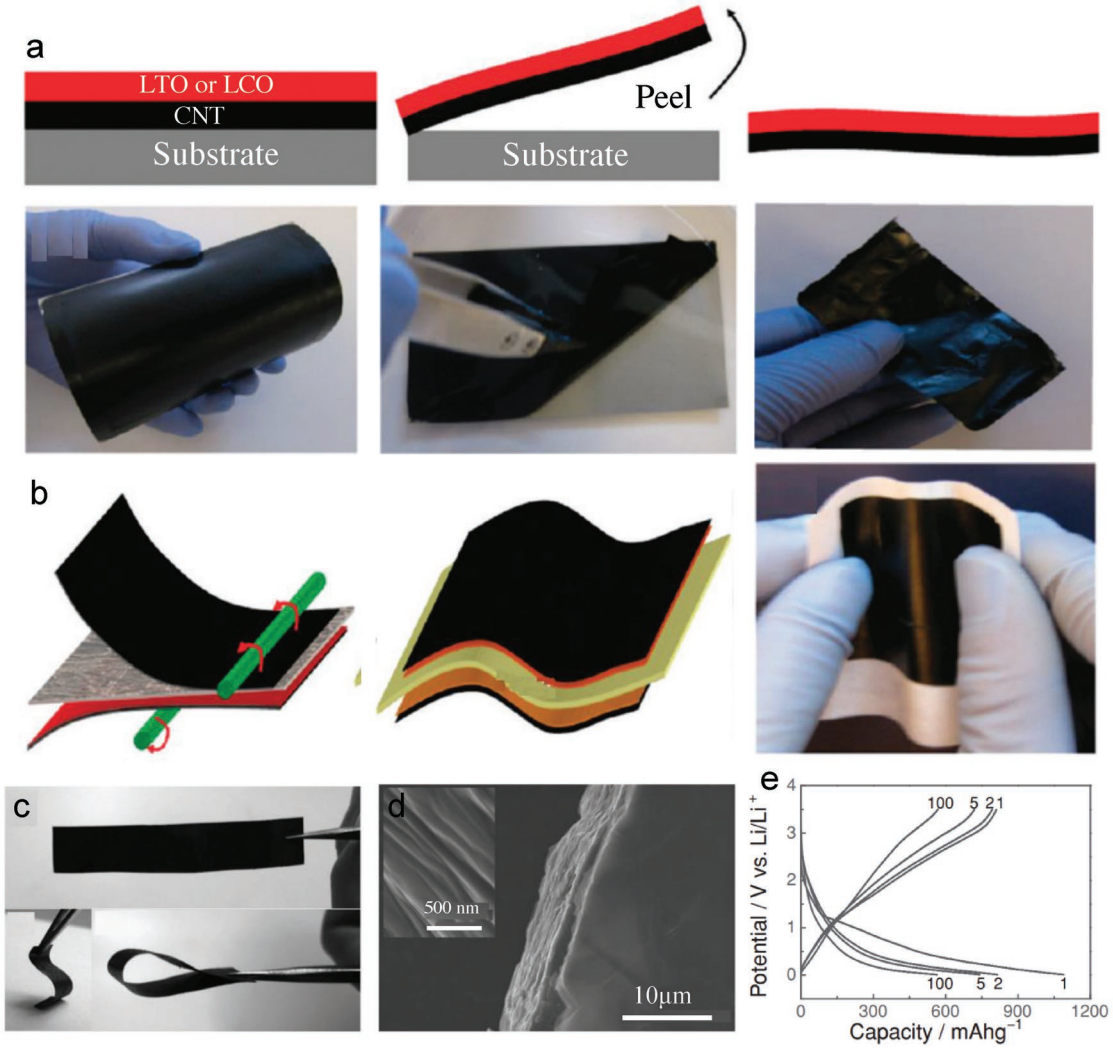

Figure 11. Schematic of the fabrication process for freestanding LCO/CNT or LTO/CNT double-layer thin films. b) Schematic of the lamination process: the freestanding film is laminated on paper with a rod and thin layer of wet PVDF on paper, and a schematic of the final paper lithium-ion paper battery device structure and picture of the lithium-ion battery before encapsulation for measurement. a,b) Reproduced with permission.[98] Copyright 2010, American Chemical Society. c) Digital images and d) SEM images of graphene paper. e) Discharge/charge profiles of the as-prepared graphene paper as an LIB anode. c–e) Reproduced with permission.[56] Copyright 2012, Wiley-VCH.

addition, the battery in the folded state showed a slightly lower discharge capacity based on active material of 103 mAh g^{-1} than 113 mAh g^{-1} when unfolded. The present areal capacity for the completely compressed state is ≈1.2 mAh cm^{-2}, and the value can be increased by adding considerable active materials to the obtained thicker electrodes. However, such modifications may reduce the rate capacity and folding difficulty. The mass loading of the active materials was limited to ≈1 mg cm^{-2} in these studies possibly given the fragility of the Kimwipe tissues that were used as the support substrate. These mass loadings are five to tenfold lower than the industrial standard for LIBs. Moreover, the achievable energy densities of these foldable batteries were limited to ≈100 Wh kg^{-1}. The fabricated composite CNT film, composed of Kimwipe tissues, CNTs, and PVDF, also limited the assembly of the folding battery.

CNT macrofilms fabricated through the CVD method are porous and consist of entangled nanotube bundles that form an interconnected network. The microscopic morphology determines the light weight (lighter than printer paper) and excellent flexibility (can be bent and folded easily) of the as-prepared macrofilms. The manufacturing process used to produce the freestanding CNT macrofilm is easy to implement at an industrial scale. Such an interconnected network of CNTs provides channels for the mobile charge carrier and is well suited to serve as a current collector. The active materials infiltrated in the pores of the CNT macrofilm can endure much longer bending cycles, compared with the active materials coated on a conventional metallic foil. These results indicate that the interfacial bonding is stronger at the active-material/CNT-macrofilm interface than at the active-material/metallic-foil interface. Because electrode slurries cannot penetrate deeply into the surface of metallic current collectors, their durability is poor when subjected to large deformation cycles in foldable electronic devices. In addition, the roughened surfaces and nanoporous architectures

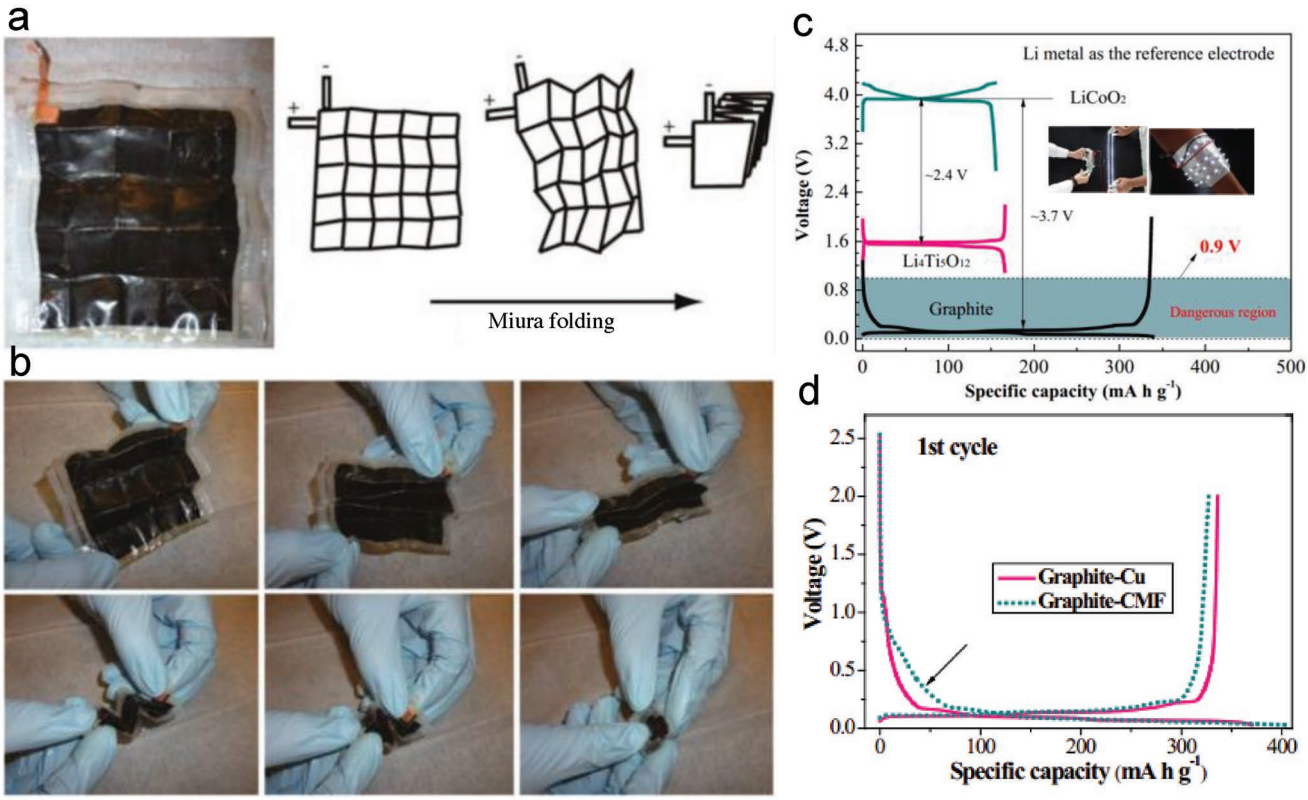

Figure 12. a) Schematic of Miura folding procedures for a 5 × 5 pattern (right) and photograph of a 6 cm × 7 cm battery sealed in parylene-C (unfolded state) (left). b) Photographs of Miura folding to compact the battery to its folded state. a,b) Reproduced with permission.[132] Copyright 2013, American Chemical Society. c) Potentials of three kinds of materials with lithium metal as the reference electrode (inset, the flexibility of the as-fabricated lithium-ion battery with paper-like structure). d) The first cycle of GPE–CMF and GPE–Cu electrodes. c,d) Reproduced with permission.[14] Copyright 2015, Elsevier.

of the CNT macrofilm also improved the interface of the current collector and the active material. The performance of the assembled battery by such electrodes is shown to be insensitive to folding. The energy density is 170 Wh kg^{-1} based on the battery, which is nearly twice the energy density of conventional LIBs that use aluminum/copper foils as the current collector.[13] The electrodes were synthesized with a high mass loading of active materials (between 5 and 13 mg cm^{-2}), thereby illustrating the mass scalability of the manufacturing process. After engineering the surface/interface of the macrofilm, horizontally oriented and ultralarge (1800 mm × 1000 mm) films can be batch-fabricated with high shape conformability and enhanced electrical conductivity.[134] When the macrofilms are used as the current collector for the cathode and anode in flexible LIBs, a wonderful flexibility and electrochemical stability with a capacity higher than 700 mAh and excellent charge/discharge rates were demonstrated. More practically, the batteries have exhibited a stable performance in variable environments, such as in a hot summer, a cold winter, or a vacuum state.

Wallace and co-workers[135] first investigated the LIB performance of graphene paper. However, the capacity of graphene paper remained unsatisfactory, and the capacity decayed severely due to the irreversible embedded lithium process. Zhang et al.[56] reported a novel approach to fabricate graphene paper with folded structured graphene sheets by freeze-drying a GO aqueous dispersion and subsequent thermal reduction (Figure 11c,d). This kind of graphene paper can show significantly improved performances, as shown in Figure 11e, such as bieng more flexible, binder-free, freestanding, and suitable for mass production, when used as the electrodes for an LIB compared with other available carbon materials. Many researchers have introduced numerous pores into graphene films to improve the capacity. Niu et al.[136] used an autoclaved foaming strategy to prepare porous rGO foams. This porous rGO foam showed higher specific capacitance than compact graphene films. The existence of graphene sheet folding can also enhance the accessibility of lithium ions and electrolytes, thereby demonstrating a better performance than graphene films fabricated through a flow-directed assembly method.

Graphene-based composite materials are predicted to be effective and practical electrodes to utilize all the potential advantages of graphene in LIBs.[15,137–139] In a composite, graphene provides chemical functionality and compatibility to allow easy processing of metal oxides in the composite. The metal oxide component mainly provides a high capacity depending on its structure, size, and crystallinity. The resultant composite is a new material with new functionalities and properties, rather than the sum of the individual components. Significant synergistic effects frequently occur in graphene/metal oxide composites, considering size effects and interfacial interactions. Many graphene/metal oxide composites, such as SnO_2,[140] Co_3O_4,[141] Fe_2O_3,[142] TiO_2,[143] and $LiFePO_4$,[144]

have been suggested. The functions and synergistic effects of graphene and metal oxides in graphene/metal oxide composites are summarized as follows: i) graphene is a 2D support to uniformly anchor or disperse metal oxides with well-defined sizes, shapes, and crystallinity; ii) metal oxides suppress the restacking of graphene; iii) graphene acts as a 2D conductive template or builds a 3D conductive porous network to improve the poor electrical properties and charge-transfer pathways of pure oxides; iv) graphene suppresses the volume change and agglomeration of metal oxides.

As stated previously, metal current collectors are a major limiting factor for flexible LIBs, in contrast, graphene has a low density and improved flexibility. Therefore, graphene can also be considered as a current collector, and the active materials are loaded through the traditional slurry-coating method.[145] Shi et al.[146] deposited active materials on a highly conductive graphene membrane through a two-step filtration method. Graphene paper anodes typically experience a large irreversible capacity, low initial efficiency, and fast capacity fading. This condition is mainly due to the restacking of the graphene sheets and side reactions between the graphene and the electrolyte that emerge from the functional groups and defects of graphene sheets. A unique 3D graphene macroscopic structure, namely, graphene foam, was prepared, and a thin, lightweight, and flexible LIB made from graphene foam was used as a current collector loaded with LTO and $LiFePO_4$ for use as the anode and cathode, respectively;[147] graphene foam is a 3D, flexible, and conductive interconnected network. The flexible complete LIB exhibited a high rate performance and energy density, and could be repeatedly bent to a radius of 5 mm without structural failure and performance loss. These electrodes displayed stronger adhesion, better electrochemical performance, higher energy density, and better flexibility than conventional electrodes that use metal as current collectors.

In the aforementioned reports, the selection of the anode materials, including $ZnCo_2O_4$ nanowire arrays,[148] Fe_2N nanoparticles,[149] red phosphorous,[150] mesoporous and nanostructured TiO_2 layers,[151] metal–organic framework (MOF)-derived materials,[152] 3D CNT/graphene structures,[153] 3D nitrogen-doped graphene foam with encapsulated germanium/nitrogen-doped graphene yolk–shell nanoarchitectures,[154] 3D carbon nanostructures of vertically aligned CNT arrays grown on carbon-cloth-actualized thick Si film,[155] biological materials coated with CNTs or graphene,[156] and heat-treated CNTs as active materials,[157] displayed diversity. LTO is a popular anode involved in flexible or foldable LIBs based on two carbon current collectors. Wu and co-workers[14] demonstrated that a potential threshold exists for selecting active materials, especially anodes for flexible or foldable LIBs using CNT current collectors, and the results can be seen in Figure 12c,d. CNT macrofilms can be used for loading most of the present cathode materials, such as $LiNi_{0.5}Mn_{1.5}O_4$,[158] $LiNi_{0.75}Co_{0.11}Mn_{0.14}O_2$ particles,[159] and polyimide,[160] because the potential of the majority of available cathode materials is higher than 3.4 V (vs Li/Li^+). However, a potential threshold exists for anode materials to match CNT current collectors. If the anode material has a potential higher than 0.9 V (vs Li/Li^+), then a favorable performance of CNT-based foldable LIBs will be obtained, because the Li^+ passes the potential threshold and the CNTs retain their electrochemical inactivity. However, if the potential of the anode is lower than 0.9 V (vs Li/Li^+), then numerous free Li^+ ions will be constrained and will mainly form Li_2CO_3. Accordingly, the capacity of CNT-based electrodes will be reduced, and the cycling performance will be poor.

Generally, the electrodes of the 1D cable LIBs will be packaged by a heat-shrinkable tube, and the force generated by the shrinking of the heat-shrinkable tube will make the structure of the cathode-electrode/separator/anode-electrode tight. Meanwhile, the 2D flexible LIB is in a planar sandwich structure instead of a tubular structure, where the packaging force will be provided between electrodes. Therefore, improving the mechanical contact between the active materials and the current collector in 2D LIBs is more important than that in 1D LIBs. The CNT networks formed by entangled nanotube bundles will induce strong adhesion between the current collectors and the active materials. The pores formed by stacking different graphene sheets will also improve the adhesion of the contact interface. Meanwhile, the contact resistance between the carbon nanomaterials and the active materials can also be improved, and the electronic current can be transferred to the external circuit more easily if the electronic conductivity of the CNTs and graphene can be increased further.

3.2.2. 2D Flexible Lithium–Sulfur Batteries

In addition to LIBs, lithium–sulfur batteries with a paper-like structure based on carbon nanomaterials have also been investigated.[161–164] Xu and co-workers[165] prepared compact, flexible, and freestanding films with a sandwich structure that was simply designed by vacuum filtration, in which nanosulfur was homogenously coated by graphene and poly(3,4-ethylene-dioxythiophene):poly(styrenesulfonate) (PEDOT:PSS). This unique hierarchical structure provides a highly conductive network and intimate contacts between the nanosulfur and the graphene/PEDOT:PSS for effective charge transportation and offers synergistic physical restriction and chemical confinement of dissoluble intermediate lithium polysulfides during the electrochemical processes. Therefore, these conductive compact films, which are used directly as cathodes, show a high reversible volumetric capacity, remarkable rate performance, and excellent mechanical properties at different bending radii. Koratkar and co-workers reported a fully foldable lithium–sulfur battery using a CNT-macrofilm-coated sulfur-containing slurry.[166] The plasticity of lithium metal during the folding/unfolding process is another main obstacle to achieving a foldable lithium–sulfur battery. The obstacle was solved by using a mask in a checkerboard pattern to make lithium squares on the CNT macrofilm (**Figure 13**a,b). Thereby, an excellent flexibility of the lithium–sulfur battery can be obtained, as shown in Figure 13c–f. The mass loading of sulfur can reach 6.8 mg cm^{-2}. Thus, the areal capacity improved to 3 mAh cm^{-2}, and the battery showed less than 12% loss in specific capacity over 100 continuous folding and unfolding (Figure 13g,h). CNTs that interpenetrate the MOF crystal on a molecular scale with abundant porosity have also been explored in terms of loading sulfur to assemble a lithium–sulfur battery with flexibility.[167] Low

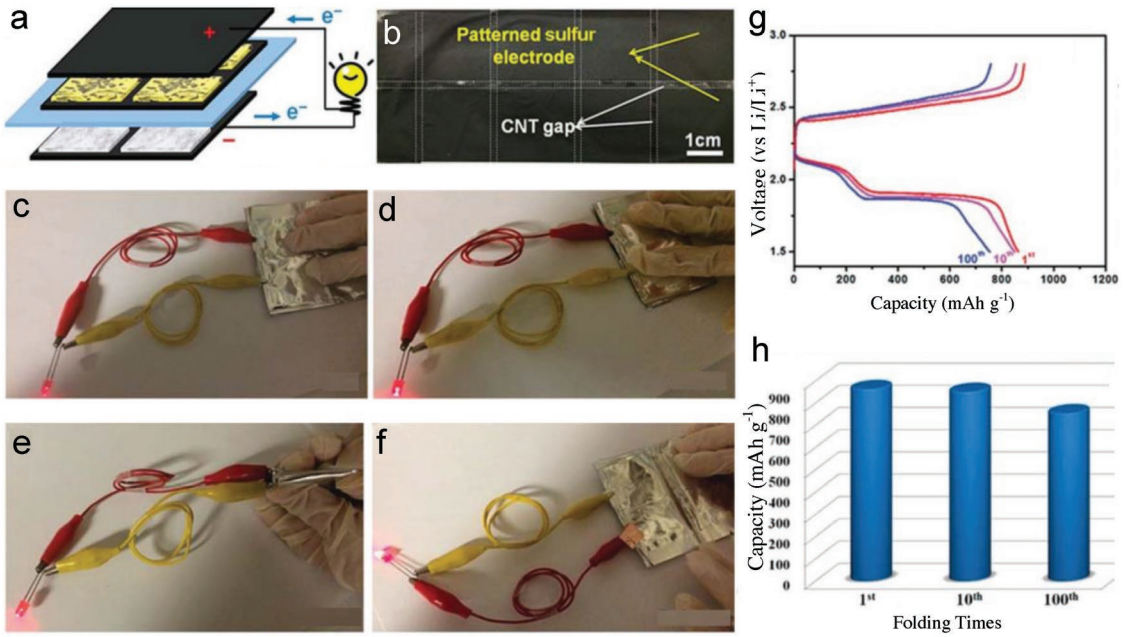

Figure 13. a) Schematic of prototype foldable lithium–sulfur battery with the active materials patterned into the CNT current collector films in a checkerboard pattern. b) Photograph showing patterning of sulfur into the CNT current collector. c–f) Qualitative demonstration of the insensitivity on the folding processes of the battery by checking the LED illumination. g) Galvanostatic charge/discharge curves of the prototype foldable lithium–sulfur battery after 1, 10, and 100 folding/unfolding cycles. h) Specific capacity of the foldable battery after 1, 10, and 100 folding/unfolding cycles at a charge/discharge rate of 0.5 C. a–h) Reproduced with permission.[166] Copyright 2015, American Chemical Society.

sulfur utilization, pore reaction kinetics, and fast capacity fading have been solved;[168,169] thus, a long-term galvanostatic cycling of 200 cycles showed an areal capacity of 3.5 mAh cm^{-2} with a sulfur loading of 4.57 mg cm^{-2} after activation in the first few cycles and remained stable during the subsequent cycles under different bending angles. Graphene has also been applied to fabricate lithium–sulfur batteries. Xiao and co-workers[161] reported a sandwich structure with nanosulfur that was homogenously coated by graphene, which provided a high conductive network and intimate contacts between sulfur and graphene for effective charge transportation. No cracks could be found after the electrode had been bent. The structure demonstrated reversible volumetric capacities of 1432 Ah L^{-1} at 0.1 C and 1038 Ah L^{-1} at 1 C, and cycling stability with a minimal decay rate of 0.04% per cycle over 500 cycles at 1 C. Certain 3D carbon nanomaterials, such as MgO-decorated carbon foam@CNTs,[170] graphene foam composited with sulfur nanoparticles,[171] and many others[172] have been used for flexible lithium–sulfur batteries, and have shown stable electrochemical characteristics under bending and folding.

Like 2D flexible LIBs, CNTs and graphene used as supports in flexible lithium–sulfur batteries with paper-like structure could provide high contact strength and resistance between the carbon nanomaterials and sulfur. A flexible sulfur electrode and effective charge transportation can thus be obtained. The porosity and electronic conductivity of the CNTs and graphene will affect the electrochemical performance of flexible batteries significantly. However, the current mass loading of sulfur on carbon nanomaterials is not enough for practical applications, in addition to the challenges of using lithium metal in wearables.

3.2.3. Other 2D Flexible-Type Batteries

Lithium–air batteries have emerged as a promising candidate considering their ultrahigh theoretical energy density.[173,174] Paper–ink[175] or TiO_2 nanowire arrays[176] as the air cathode, and lithium foil as the anode have been assembled to prepare lithium–air batteries. New structures have also been explored for flexible lithium–air battery, such as the bamboo slip architecture.[177] Many other strategies for the battery based on carbon nanomaterials for flexibility have also been developed. Jiang et al.[178] reported graphene foam decorated with ceria microspheres as a flexible cathode for foldable lithium–air batteries. However, the lithium-foil anodes in these studies limited the flexibility of the battery. Liu et al.[179] reported a "break-up-the-whole-into-parts" system to build a segmented lithium–air battery to avoid the cracks generated after repetitive folding or bending that would inevitably lead to poor robustness and short circuit. CNTs are used to confine the cathode (ruthenium dioxide) inside their channels. The flexible lithium–air battery showed gravimetric and volumetric energy densities of 294.68 Wh kg^{-1} and 274.06 Wh L^{-1}, which were calculated based on the weight and volume of the whole device, correspondingly. The flexibility of the battery was achieved in 10 000 cycles of folding/stretching.

Rechargeable lithium–carbon-dioxide batteries with flexible and 2D structures have also been fabricated by lithium foil and wrapping cross-stacked CNTs that loaded methacrylate and ethylene glycol composite as the air cathode.[180] The assembled battery ran for 100 cycles with a fixed capacity and an energy density of 1000 mAh g^{-1} and 521 Wh kg^{-1}, respectively, based on the whole battery. A total of 220 h operation at 0–360°

bendable gestures were obtained. In addition, rechargeable aluminum-ion batteries with a 2D structure for wearable electronics have been investigated.[181] CNT was used to encapsulate cobalt sulfide as a cathode electrode. The optimized electrode exhibited a capacity of 315 mAh g^{-1} at 100 mA g^{-1} and cycling stability of 297 mAh g^{-1} at 100 mA g^{-1} after 200 cycles. Graphene supporting red-phosphorus nanodots[182] or other nanodots[183,184] has been examined to fabricate flexible sodium-ion batteries with a paper-like structure. One of the main issues regarding application of CNTs in batteries is the contact strength and resistance between the carbon nanomaterial and active materials. Another important factor that should be considered is the mass loading of the active materials on the CNTs. Graphene enhances the electrical conductivity and facilitates electron transport in the electrodes. With the porosity between the graphene flakes, the contact interface between the current collector and the active materials can also be strengthened. Therefore, the anode delivered a long cycling stability with a reversible capacity of 56.3 mAh g^{-1} at 1 A g^{-1} after 5000 cycles. Other types of flexible batteries based on carbon nanomaterials, such as sodium–sulfur batteries using carbon nanofibers binding sulfur as an electrode,[185] zinc–air batteries using carbon films as electrodes,[186] and zinc–carbon batteries using carbon nanofiber mats as the current collector[187] for 2D structures, have also been investigated. A major obstacle to achieve flexible or wearable batteries is using metal-foil anodes.[138] Metallic foils have low elastic strain and fatigue during repeated bending or folding. The application of metal-free anodes or other strategies should be developed to solve this issue.

As previously discussed, different types of flexible batteries with a 2D structure based on carbon nanomaterials have been studied.[188] Due to the characteristics of flexible electrodes with a 2D structure based on carbon nanomaterials, the corresponding battery will be lightweight and small in size, thereby providing flexibility, and facilitating the development of electronic devices with different functionalities. **Table 2** summarizes the recent studies of the performance of the flexible batteries with a 2D structure based on carbon nanomaterials. The different types of flexible batteries that serve as a new kind of power source show promising applications with the huge demand for flexible electronics in the foreseeable future.

From the above flexible batteries, CNTs are current collectors in different batteries for depositing various active materials, such as MnO_2, Si, LMO, LTO, or electrocatalysts as electrodes. The electrochemical properties of the obtained batteries will be affected significantly by the electrical conductivity of the CNTs, as well as the mechanical and electrical contact between the current collector and the active materials. CNTs can also function as conductive additives, and electrons can be transferred rapidly causing increased lithium-ion insertion/extraction in batteries. In lithium–sulfur batteries, for example, CNTs have been used both as current collectors and conductive additives. In metal–air batteries, CNTs have been used as the active sites for loading catalysts for the ORR and OER, and also acted as a gas-diffusion layer to admit continuous and inexhaustible oxygen from the surrounding air to reach the three-phase boundary for reaction. Therefore, the ideal CNTs for different metal–air batteries are expected to have excellent electronic conductivity and high oxygen permeation rate. Graphene has also been used as a flexible support for loading catalyst and a gas-diffusion layer to admit air to reach the three-phase boundary. In most batteries, active materials can also be regularly stacked on graphene flakes that serve as current collectors for 1D or 2D electrodes in LIBs and lithium–sulfur batteries with excellent

Table 2. The performances of the reported 2D flexible batteries.

Battery type	Voltage [V]	Specific capacity [mAh g^{-1}]	Active material mass loading [mg cm^{-2}]	Flexibility	Energy density [Wh kg^{-1}]
LCO–CNT/LTO–CNT[98]	2.7	147	≈7	Bendable	108, based on whole battery
LCO–CMF/LTO–CMF[13]	2.7	164.3	13	Foldable	170, based on whole battery
LCO–CNT–Kimwipes/LTO–CNT–Kimwipes[132]	2.65	103	1.29	Foldable	≈100, based on electrode
LCO–Al foil/$ZnCo_2O_4$–carbon cloth[148]	3.4	1300	1–1.2	Bendable	–
LCO–Al/Fe_2N–carbon textile–Cu[149]	3	215	0.9	Bendable	688, based on active materials
$LiNi_{0.5}Mn_{1.5}O_4$–CNT/Li–Cu[158]	2.8	140	5	Bendable	–
$LiNi_{0.75}Co_{0.11}Mn_{0.14}O_2$-patterned Al/Si loaded expanded graphite-patterned-Cu[159]	3.9	185	5.3	Bendable	368, based on electrode
Li strip/S–graphene-PP[164]	2.3	985	1.5–2.1	Bendable	1100, based on electrode
Li foil/S–rGO–PEDOT:PSS[165]	2.4	1038	2	Bendable	–
Pattern Li coating-CMF/sulfur–CMF[166]	2.4	863.7	3.6	Foldable	750, based on active materials
Li foil/S@HKUST-1-CNT[167]	2.1	784.2	4.57	Bendable	–
Small lithium disks-PET/O_2–RuO_2–CNT[120]	2.5	1000	–	Bendable	294.68, based on whole battery
Lithium foil/O_2–TiO_2 NAs/CT[176]	2.5	500	–	Bendable	–
Lithium foil/O_2–C–CeO_2@graphene foam[178]	2.58	600	2	Bendable	–
Li foil/CO_2–CPE@CNT[180]	2.3	226	41.25	Bendable	521, based on whole battery
Aluminum foil/Co_9S_8@CNT–CNT[181]	1	315	1.5	Bendable	–
Zinc plate/O_2–NCNF[186]	1.2	626	2	Bendable	776, based on consumed zinc

integrated mechanical properties. High mass loading of active materials on graphene with high electronic conductivity and binder-free property will lead to a competitive energy density of the obtained batteries.

4. Conclusions and Perspectives

We have investigated the most recent progress on fabricating flexible batteries with fiber-shaped, paper-like, and foam-structured carbon nanomaterials, including CNTs, graphene, and their composite. The main role of carbon nanomaterials used in flexible batteries is to provide a conductive framework. First, CNTs and graphene function as networks to provide efficient electron-transport pathways. Moreover, porous CNTs or graphene can provide significant surface area and strong adhesion to active materials. Second, the light weight of carbon nanomaterials will reduce the weight of the entire electrodes and the battery. Third, the excellent mechanical properties of CNTs, graphene, or their composites will make electrodes flexible or even foldable. Finally, a favorable cyclic reversibility and anticorrosive performance will occur given the high chemical stability of carbon nanomaterials. The strategies can also be extended to other flexible energy-storage or electronic devices. For example, CNTs and graphene can be widely used in flexible electrodes to build flexible supercapacitors,[189–191] mechanical energy dissipation,[192,193] energy harvesters,[194–196] sensors,[197] actuators,[198] or light-emitting electrochemical cells[199] for wearable electronics. Carbon nanomaterials may eventually become the general manufacturing materials from which to produce flexible batteries.

Although significant achievements have been demonstrated in the past years, several significant challenges of carbon nanomaterials still exist in flexible batteries. Carbon nanomaterials, such as CNTs or graphene with fiber, film, or sponge morphologies, can be easily fabricated in the laboratory for assembling various prototypes of flexible batteries. However, it remains difficult to produce macroscopic carbon nanomaterials on a large scale, and it is hard to control their morphology by present technologies. In addition, carbon nanomaterials cannot be fabricated using rolls. Therefore, they are not adapted to the modern battery production process. Carbonaceous nanomaterials exhibit favorable electrical conductivity and excellent mechanic properties in an ideal situation. However, their actual electrical conductivity may be inferior to traditional metals, such as the copper and aluminum foils commonly used in LIBs. This will result in an increased internal resistance, and a deteriorated electrochemical performance of the batteries. Moreover, the current coating or depositing technologies are developed for rigid current collectors or supports, and are not adapted to flexible carbon nanomaterials for loading active materials.

The electrochemical and mechanical performances of the electrodes and degradation of the interfacial properties between the electrode materials and current collector under structure change of the whole battery will also influence the performance of the batteries. Currently, the specific capacity of the most flexible batteries with carbon nanomaterials is calculated based on the weight of active materials, while the electrolyte, current collector, separator, and packaging are not included. Therefore, the electrochemical performances of the electrodes should be increased further for most practical applications. On the other hand, the mechanical performances of the electrodes will deteriorate with high mass loading of active materials on current collectors, and the flexibility of the electrode will also be decreased. Moreover, the adhesion between the active materials and current collectors will also be degraded, especially on structure-changing states. Therefore, considerable attention should be focused on appropriate surface morphologies of the carbon nanomaterials for loading more active materials.

The elastic strain of metal foils during the folding/unfolding process is another main obstacle to achieve flexible metal–air batteries. Metal cracks will be generated after repetitive folding or bending that will inevitably lead to poor robustness and short circuit. In addition, the gravimetric and volumetric energy densities will be reduced considering the increase in weight and volume when metals are used. Other challenges similar to rigid batteries, such as a stable solid electrolyte interphase (SEI) for the anode and cathode electrolyte interphase (CEI) for the cathode, and lithium-dendrite formation will be worse in flexible batteries. The SEI allows lithium-ion transport and blocks electrons in order to prevent further electrolyte decomposition and ensure continued electrochemical reactions. Capacity decay will occur when the CEI resistance between the cathode and the current collectors increases. The problems related to lithium-dendrite growth such as capacity loss and short circuit are also major barriers to flexible batteries with high energy density. Therefore, the strategies for appropriate formation and growth of SEI, CEI, and lithium dendrites should be investigated further.

Safety is also a critical issue for batteries, especially for flexible batteries mounted on human bodies. Liquid electrolytes are applied in most current flexible batteries, and the obtained batteries are facing several inherent limitations of leakage, flammability, and volatility of the electrolytes. Therefore, the battery packages are one of the most technically complicated tasks in the field of battery materials. Some reported 1D flexible batteries packaged by a heat-shrinkable tube can work normally no longer than one month due to the evaporation of the electrolyte. The aluminum plastic film, which mainly consists of a nylon layer, then an aluminum foil layer, and a polypropylene layer, has high barrier properties, good heat-sealing performance, and good ductility, flexibility, and mechanical strength. Due to the barrier properties and mechanical strength of aluminum foil, the liquid electrolyte cannot easily infiltrate into the inner layer of the aluminum plastic film. Hence, it is an ideal packaging material for batteries. However, the aluminum foil cannot be fabricated thin enough to accommodate the flexibility of the flexible batteries. Therefore, it is urgent to develop thin and light materials with excellent barrier and high mechanical strength.

Solid electrolytes can not only address safety concerns of leakage, flammability, and volatility of liquid electrolytes, but also enable the use of high-voltage cathode materials and low-potential anodes to allow high-energy-density and long-term stable batteries. Thereby the aluminum plastic films can be replaced by more flexible and thinner packages. In addition, the flexibility and energy density of the obtained batteries will be increased. Currently, the relatively low electrical conductivity of most solid electrolytes and the inefficient charge-transfer

kinetics at the interface between the solid electrolyte and the different electrode layers are the major challenges facing batteries based on solid electrolytes. Therefore, extensive studies will be necessary to develop a solid electrolyte with high ionic conductivity at low temperature, in a wide electrochemical window, and with excellent Young's modulus.

In conclusion, carbon nanomaterials present excellent advantages, such as flexibility and light weight, compared with the traditional materials in batteries. However, the performance of flexible batteries used in wearable electronics needs to be improved to meet the requirements of power-hungry electronic devices. The development of flexible batteries will cover various subjects, including materials, chemistry, physics, and engineering, etc. We believe that future flexible power sources, combining excellent mechanical performance and outstanding electrochemical properties, will lead to many advances in technology and boost the development and commercialization of wearable electronics given the rapid progress in technologies and material engineering. Many disruptive technologies could be incubated from flexible batteries. It can be foreseen in the near future; sensors powered by flexible batteries can be mounted on the skin or clothes, harvesting reams of data, transforming health care, and creating an incredible amount of convenience in our daily lives.

Acknowledgements

This work was financially supported by the National Basic Research Program of China. (Nos. 2016YFA0200101 and 2014CB932500), the National Natural Science Foundation of China (Nos. 51432002, 51520105003, 51362029, 51202095, 51861009, and 51264010), the Department of Science and Technology of Jiangxi Province (20153BCB23011, GJJ150617, GJJ160596, 20171ACB21043), and the program for Excellent Young Talents, JXUST.

Conflict of Interest

The authors declare no conflict of interest.

Keywords

carbon nanomaterials, carbon nanotubes, flexible batteries, graphene

Received: February 1, 2018
Revised: December 3, 2018
Published online: January 25, 2019

[1] J. Bardeen, W. H. Brattain, *Phys. Rev.* **1948**, *74*, 230.
[2] H. J. Peng, J. Q. Huang, Q. Zhang, *Chem. Soc. Rev.* **2017**, *46*, 5237.
[3] T. Chen, L. B. Qiu, Z. B. Yang, Z. B. Cai, J. Ren, H. P. Li, H. J. Lin, X. M. Sun, H. S. Peng, *Angew. Chem., Int. Ed.* **2012**, *51*, 11977.
[4] Z. T. Zhang, X. L. Chen, P. N. Chen, G. Z. Guan, L. B. Qiu, H. J. Lin, Z. B. Yang, W. Y. Bai, Y. F. Luo, H. S. Peng, *Adv. Mater.* **2014**, *26*, 466.
[5] Z. B. Yang, T. Chen, R. X. He, G. Z. Guan, H. P. Li, L. B. Qiu, H. S. Peng, *Adv. Mater.* **2011**, *23*, 5436.
[6] P. Tan, B. Chen, H. R. Xu, H. C. Zhang, W. Z. Cai, M. Ni, M. L. Liu, Z. P. Shao, *Energy Environ. Sci.* **2017**, *10*, 2056.
[7] Y. Q. Liu, K. He, G. Chen, W. R. Leow, X. D. Chen, *Chem. Rev.* **2017**, *117*, 12893.
[8] L. M. Sun, X. H. Wang, Y. R. Wang, Q. Zhang, *Carbon* **2017**, *122*, 462.
[9] Q. Y. Huang, D. R. Wang, Z. J. Zheng, *Adv. Energy Mater.* **2016**, *6*, 1600783.
[10] L. L. Peng, Y. Zhu, H. S. Li, G. H. Yu, *Small* **2016**, *12*, 6183.
[11] C. F. Du, Q. H. Liang, Y. B. Luo, Y. Zheng, Q. Y. Yan, *J. Mater. Chem. A* **2017**, *5*, 22442.
[12] H. Nishide, K. Oyaizu, *Science* **2008**, *319*, 737.
[13] J. W. Hu, Z. P. Wu, S. W. Zhong, W. B. Zhang, S. Suresh, A. Mehta, N. Koratkar, *Carbon* **2015**, *87*, 292.
[14] Q. H. Wang, S. W. Zhong, J. W. Hu, T. Liu, X. Y. Zhu, J. Chen, Y. Y. Hong, Z. P. Wu, *J. Power Sources* **2016**, *310*, 70.
[15] Y. Zhang, Y. D. Jiao, M. Liao, B. J. Wang, H. S. Peng, *Carbon* **2017**, *124*, 79.
[16] G. M. Zhou, F. Li, H. M. Cheng, *Energy Environ. Sci.* **2014**, *7*, 1307.
[17] B. J. Landi, M. J. Ganter, C. D. Cress, R. A. DiLeo, R. P. Raffaelle, *Energy Environ. Sci.* **2009**, *2*, 638.
[18] Z. B. Yang, J. Deng, X. L. Chen, J. Ren, H. S. Peng, *Angew. Chem., Int. Ed.* **2013**, *52*, 13453.
[19] J. Ren, W. Y. Bai, G. Z. Guan, Y. Zhang, H. S. Peng, *Adv. Mater.* **2013**, *25*, 5965.
[20] X. L. Chen, L. B. Qiu, J. Ren, G. Z. Guan, H. J. Lin, Z. T. Zhang, P. N. Chen, Y. G. Wang, H. S. Peng, *Adv. Mater.* **2013**, *25*, 6436.
[21] H. W. Zhu, C. L. Xu, D. H. Wu, B. Q. Wei, R. Vajtai, P. M. Ajayan, *Science* **2002**, *296*, 884.
[22] M. Endo, H. Muramatsu, T. Hayashi, Y. A. Kim, M. Terrones, M. S. Dresselhaust, *Nature* **2005**, *433*, 476.
[23] X. C. Gui, J. Q. Wei, K. L. Wang, A. Y. Cao, H. W. Zhu, Y. Jia, Q. K. Shu, D. H. Wu, *Adv. Mater.* **2010**, *22*, 617.
[24] Z. Xu, Y. J. Liu, X. L. Zhao, L. Peng, H. Y. Sun, Y. Xu, X. B. Ren, C. H. Jin, P. Xu, M. Wang, C. Gao, *Adv. Mater.* **2016**, *28*, 6449.
[25] D. A. Dikin, S. Stankovich, E. J. Zimney, R. D. Piner, G. H. B. Dommett, G. Evmenenko, S. T. Nguyen, R. S. Ruoff, *Nature* **2007**, *448*, 457.
[26] M. Zhang, L. Huang, J. Chen, C. Li, G. Shi, *Adv. Mater.* **2014**, *26*, 7588.
[27] H. Hu, Z. B. Zhao, W. B. Wan, Y. Gogotsi, J. S. Qiu, *Adv. Mater.* **2013**, *25*, 2219.
[28] F. C. Meng, R. Li, Q. W. Li, W. B. Lu, T. W. Chou, *Carbon* **2014**, *72*, 250.
[29] X. C. Dong, B. Li, A. Wei, X. H. Cao, M. B. Chan-Park, H. Zhang, L. J. Li, W. Huang, P. Chen, *Carbon* **2011**, *49*, 2944.
[30] W. C. Wan, R. Y. Zhang, W. Li, H. Liu, Y. H. Lin, L. N. Li, Y. Zhou, *Environ. Sci.: Nano* **2016**, *3*, 107.
[31] P. M. Ajayan, J. M. Tour, *Nature* **2007**, *447*, 1066.
[32] K. V. Raman, A. M. Kamerbeek, A. Mukherjee, N. Atodiresei, T. K. Sen, P. Lazic, V. Caciuc, R. Michel, D. Stalke, S. K. Mandal, S. Blugel, M. Munzenberg, J. S. Moodera, *Nature* **2013**, *493*, 509.
[33] H. T. Sun, L. Mei, J. F. Liang, Z. P. Zhao, C. Lee, H. L. Fei, M. N. Ding, J. Lau, M. F. Li, C. Wang, X. Xu, G. L. Hao, B. Papandrea, I. Shakir, B. Dunn, Y. Huang, X. F. Duan, *Science* **2017**, *356*, 599.
[34] Z. Yuan, H. J. Peng, J. Q. Huang, X. Y. Liu, D. W. Wang, X. B. Cheng, Q. Zhang, *Adv. Funct. Mater.* **2014**, *24*, 6105.
[35] B. S. Shim, W. Chen, C. Doty, C. L. Xu, N. A. Kotov, *Nano Lett.* **2008**, *8*, 4151.
[36] K. Kang, K. H. Lee, Y. M. Han, H. Gao, S. E. Xie, D. A. Muller, J. Park, *Nature* **2017**, *550*, 229.
[37] K. S. Novoselov, A. K. Geim, S. V. Morozov, *Science* **2004**, *306*, 666.
[38] H. G. Wang, W. Li, D. P. Liu, X. L. Feng, J. Wang, X. Y. Yang, X. B. Zhang, Y. J. Zhu, Y. Zhang, *Adv. Mater.* **2017**, *29*, 1703012.

[39] S. Ijjima, *Nature* **1991**, *354*, 56.
[40] B. Vigolo, A. Pénicaud, C. Coulon, C. Sauder, R. Pailler, C. Journet, P. Bernier, P. Poulin, *Science* **2000**, *290*, 1331.
[41] N. Behabtu, C. C. Young, D. E. Tsentalovich, O. Kleinerman, X. Wang, A. W. K. Ma, E. A. Bengio, R. F. ter Waarbeek, J. J. de Jong, R. E. Hoogerwerf, S. B. Fairchild, J. B. Ferguson, B. Maruyama, J. Kono, Y. Talmon, Y. Cohen, M. J. Otto, M. Pasquali, *Science* **2013**, *339*, 182.
[42] K. L. Jiang, Q. Q. Li, S. S. Fan, *Nature* **2002**, *419*, 801.
[43] M. Zhang, K. R. Atkinson, R. H. Baughman, *Science* **2004**, *306*, 1358.
[44] B. J. Han, T. Liu, Z. J. Huang, D. M. Chen, Y. S. Zhu, C. Y. Zhou, Y. S. Li, Y. H. Yin, Z. P. Wu, *Appl. Phys. Lett.* **2017**, *110*, 103902.
[45] Q. Cao, J. A. Rogers, *Adv. Mater.* **2009**, *21*, 29.
[46] Q. F. Liu, T. Fujigaya, H. M. Cheng, N. Nakashima, *J. Am. Chem. Soc.* **2010**, *132*, 16581.
[47] J. W. Jo, J. W. Jung, J. U. Lee, W. H. Jo, *ACS Nano* **2010**, *4*, 5382.
[48] L. Xiao, Z. Chen, C. Feng, L. Liu, Z. Q. Bai, Y. Wang, L. Qian, Y. Y. Zhang, Q. Q. Li, K. L. Jiang, S. S. Fan, *Nano Lett.* **2008**, *8*, 4539.
[49] Q. W. Li, X. F. Zhang, R. F. DePaula, L. X. Zheng, Y. H. Zhao, L. Stan, T. G. Holesinger, P. N. Arendt, D. E. Peterson, Y. T. Zhu, *Adv. Mater.* **2006**, *18*, 3160.
[50] Y. H. Li, Y. M. Zhao, M. Roe, D. Furniss, Y. Q. Zhu, S. R. P. Silva, J. Q. Wei, D. H. Wu, C. H. P. Poa, *Small* **2006**, *2*, 1026.
[51] W. J. Ma, L. Song, R. Yang, T. H. Zhang, Y. C. Zhao, L. F. Sun, Y. Ren, D. F. Liu, L. F. Liu, J. Shen, Z. X. Zhang, Y. J. Xiang, W. Y. Zhou, S. S. Xie, *Nano Lett.* **2007**, *7*, 2307.
[52] K. Koziol, J. Vilatela, A. Moisala, M. Motta, P. Cunniff, M. Sennett, A. Windle, *Science* **2007**, *318*, 1892.
[53] W. Xu, Y. Chen, H. Zhan, J. N. Wang, *Nano Lett.* **2016**, *16*, 946.
[54] P. Simon, Y. Gogotsi, B. Dunn, *Science* **2014**, *343*, 1210.
[55] M. Z. Wang, M Tang, S. L. Chen, H. N. Ci, K. X. Wang, L. R. Shi, L. Li, H. Y. Ren, J. Y. Shan, P. Gao, Z. F. Liu, H. L. Peng, *Adv. Mater.* **2017**, *29*, 1703882.
[56] F. Liu, S. Y. Song, D. F. Xue, H. J. Zhang, *Adv. Mater.* **2012**, *24*, 1089.
[57] K. S. Novoselov, A. K. Geim, S. V. Morozov, D. Jiang, Y. Zhang, S. V. Dubonos, I. V. Grigorieva, A. A. Firsov, *Science* **2004**, *306*, 666.
[58] K. I. Bolotin, K. J. Sikes, Z. Jiang, M. Klima, G. Fudenberg, J. Hone, P. Kim, H. L. Stormer, *Solid State Commun.* **2008**, *146*, 351.
[59] R. Raccichini, A. Varzi, D. Wei, S. Passerini, *Adv. Mater.* **2017**, *29*, 1603421.
[60] S. V. Morozov, K. S. Novoselov, M. I. Katsnelson, F. Schedin, D. C. Elias, J. A. Jaszczak, A. K. Geim, *Phys. Rev. Lett.* **2008**, *100*, 016602.
[61] D. C. Marcano, D. V. Kosynkin, J. M. Berlin, A. Sinitskii, Z. Z. Sun, A. Slesarev, L. B. Alemany, W. Lu, J. M. Tour, *ACS Nano* **2010**, *4*, 4806.
[62] W. F. Zhao, M. Fang, F. R. Wu, H. Wu, L. W. Wang, G. H. Chen, *J. Mater. Chem.* **2010**, *20*, 5817.
[63] M. Yi, Z. G. Shen, *J. Mater. Chem. A* **2015**, *3*, 11700.
[64] K. Yan, L. Fu, H. L. Peng, Z. F. Liu, *Acc. Chem. Res.* **2013**, *46*, 2263.
[65] S. Bae, H. Kim, Y. Lee, X. F. Xu, J. S. Park, Y. Zheng, J. Balakrishnan, T. Lei, H. R. Kim, Y. I. Song, Y. J. Kim, K. S. Kim, B. Ozyilmaz, J. H. Ahn, B. H. Hong, S. Iijima, *Nat. Nanotechnol.* **2010**, *5*, 574.
[66] X. L. Wang, H. Bai, G. Q. Shi, *J. Am. Chem. Soc.* **2011**, *133*, 6338.
[67] Z. Xu, C. Gao, *Nat. Commun.* **2011**, *2*, 571.
[68] Z. L. Dong, C. C. Jiang, H. H. Cheng, Y. Zhao, G. Q. Shi, L. Jiang, L. T. Qu, *Adv. Mater.* **2012**, *24*, 1856.
[69] H. Y. Wang, G. M. Wang, Y. C. Ling, F. Qian, Y. Song, X. H. Lu, S. W. Chen, Y. X. Tong, Y. Li, *Nanoscale* **2013**, *5*, 10283.
[70] J. Ge, H. B. Yao, W. Hu, X. F. Yu, Y. X. Yan, L. B. Mao, H. H. Li, S. S. Li, S. H. Yu, *Nano Energy* **2013**, *2*, 505.
[71] W. F. Chen, Y. X. Huang, D. B. Li, H. Q. Yu, L. F. Yan, *RSC Adv.* **2014**, *4*, 21619.
[72] F. Liu, T. S. Seo, *Adv. Funct. Mater.* **2010**, *20*, 1930.
[73] Y. Xu, K. Sheng, C. Li, G Shi, *Adv. Mater.* **2013**, *25*, 2219.
[74] L. Zhang, G. Q. Shi, *J. Phys. Chem. C* **2011**, *115*, 17206.
[75] M. A. Worsley, P. J. Pauzauskie, T. Y. Olson, J. Biener, J. H. Satcher, T. F. Baumann, *J. Am. Chem. Soc.* **2010**, *132*, 14067.
[76] Z. Xu, Y. Zhang, P. G. Li, C. Gao, *ACS Nano* **2012**, *6*, 7103.
[77] Y. X. Xu, K. X. Sheng, C. Li, G. Q. Shi, *ACS Nano* **2010**, *4*, 4324.
[78] L. Qiu, D. Y. Liu, Y. F. Wang, C. Cheng, K. Zhou, J. Ding, V. T. Truong, D. Li, *Adv. Mater.* **2014**, *26*, 3333.
[79] K. Chen, C. Li, L. Shi, T. Gao, X. Song, A. Bachmatiuk, Z. Zou, B. Deng, Q. Ji, D. Ma, *Nat. Commun.* **2016**, *7*, 13440.
[80] G. K. Dimitrakakis, E. Tylianakis, G. E. Froudakis, *Nano Lett.* **2008**, *8*, 3166.
[81] F. D. Novaes, R. Rurali, P. Ordejon, *ACS Nano* **2010**, *4*, 7596.
[82] Y. H. Xue, Y. Ding, J. B. Niu, Z. H. Xia, A. Roy, H. Chen, J. Qu, Z. L. Wang, L. M. Dai, *Sci. Adv.* **2015**, *1*, e1400198.
[83] H. Sun, X. You, J. E. Deng, X. L. Chen, Z. B. Yang, J. Ren, H. S. Peng, *Adv. Mater.* **2014**, *26*, 2868.
[84] M. Li, Z. Tang, M. Leng, J. M. Xue, *Adv. Funct. Mater.* **2014**, *24*, 7495.
[85] H. H. Cheng, Z. L. Dong, C. G. Hu, Y. Zhao, Y. Hu, L. T. Qu, N. Chen, L. M. Dai, *Nanoscale* **2013**, *5*, 3428.
[86] Q. Zhang, S. J. Yang, J. Zhang, L. Zhang, P. L. Kang, J. H. Li, J. W. Xu, H. Zhou, X. M. Song, *Nanotechnology* **2011**, *22*, 494010.
[87] B. S. Kim, K. Lee, S. Kang, S. Lee, J. B. Pyo, I. S. Choi, K. Char, J. H. Park, S. S. Lee, J. Lee, J. G. Son, *Nanoscale* **2017**, *9*, 13272.
[88] H. Y. Sun, Z. Xu, C. Gao, *Adv. Mater.* **2013**, *25*, 2554.
[89] J. Kim, S. H. Bae, M. Kotal, T. Stalbaum, K. J. Kim, I. K. Oh, *Small* **2017**, *13*, 1701314.
[90] H. Sun, Y. Zhang, J. Zhang, X. M. Sun, H. S. Peng, *Nat. Rev. Mater.* **2017**, *2*, 17023.
[91] M. D. Lima, S. L. Fang, X. Lepró, C. Lewis, R. Ovalle-Robles, J. Carretero-González, E. Castillo-Martínez, M. E. Kozlov, J. Oh, M. Rawat, C. S. Haines, M. H. Haque, V. Aare, S. Stoughton, A. A. Zakhidov, R. H. Baughman, *Science* **2011**, *331*, 51.
[92] S. S. Li, Y. H. Luo, W. Lv, W. J. Yu, S. D. Wu, P. X. Hou, Q. H. Yang, Q. B. Meng, C. Liu, H. M. Cheng, *Adv. Energy Mater.* **2011**, *1*, 486.
[93] S. L. Chou, Y. Zhao, J. Z. Wang, Z. X. Chen, H. K. Liu, S. X. Dou, *J. Phys. Chem. C* **2010**, *114*, 15862
[94] Y. X. Zeng, X. Y. Zhang, Y. Meng, M. H. Yu, J. N. Yi, Y. Q. Wu, X. H. Lu, Y. X. Tong, *Adv. Mater.* **2017**, *29*, 1700274.
[95] S. Y. Lee, K. H. Choi, W. S. Choi, Y. H. Kwon, H. R. Jung, H. C. Shin, J. Y. Kim, *Energy Environ. Sci.* **2013**, *6*, 2414.
[96] Y. Zhang, Y. Zhao, J. Ren, W. Weng, H. S. Peng, *Adv. Mater.* **2016**, *28*, 4524.
[97] Z. B. Yang, J. Ren, Z. T. Zhang, X. L. Chen, G. Z. Guan, L. B. Qin, Y. Zhang, H. S. Peng, *Chem. Rev.* **2015**, *115*, 5159.
[98] L. B. Hu, H. Wu, F. La Mantia, Y. A. Yang, Y. Cui, *ACS Nano* **2010**, *4*, 5843.
[99] J. Y. Ji, H. X. Ji, L. L. Zhang, X. Zhao, X. Bai, X. B. Fan, F. B. Zhang, R. S. Ruoff, *Adv. Mater.* **2013**, *25*, 4673.
[100] A. M. Zamarayeva, A. E. Ostfeld, M. Wang, J. K. Duey, I. Deckman, B. P. Lechene, G. Davies, D. A. Steingart, A. C. Arias, *Sci. Adv.* **2017**, *3*, e1602051.
[101] W. Weng, P. N. Chen, S. S. He, X. M. Sun, H. S. Peng, *Angew. Chem., Int. Ed.* **2016**, *55*, 6140.
[102] T. Lv, Y. Yao, N. Li, T. Chen, *Nano Today* **2016**, *11*, 644.
[103] R. F. Service, *Science* **2003**, *301*, 909.
[104] Y. H. Kwon, S. W. Woo, H. R. Jung, H. K. Yu, K. Kim, B. H. Oh, S. Ahn, S. Y. Lee, S. W. Song, J. Cho, H. C. Shin, J. Y. Kim, *Adv. Mater.* **2012**, *24*, 5192.
[105] J. Ren, L. Li, C. Chen, X. L. Chen, Z. B. Cai, L. B. Qiu, Y. G. Wang, X. R. Zhu, H. S. Peng, *Adv. Mater.* **2013**, *25*, 1155.

[106] Y. Zhang, Y. Zhao, X. Cheng, W. Weng, J. Ren, X. Fang, Y. Jiang, P. Chen, Z. Zhang, Y. Wang, H. S. Peng, *Angew. Chem., Int. Ed.* **2015**, *54*, 11177.
[107] W. Weng, Q. Sun, Y. Zhang, S. He, Q. Wu, J. Deng, X. Fang, G. Guan, J. Ren, H. Peng, *Adv. Mater.* **2015**, *27*, 1363.
[108] H. J. Lin, W. Weng, J. Ren, L. B. Qiu, Z. T. Zhang, P. N. Chen, X. L. Chen, J. Deng, Y. G. Wang, H. S. Peng, *Adv. Mater.* **2014**, *26*, 1217.
[109] W. Weng, Q. Q. Wu, Q. Sun, X. Fang, G. Z. Guan, J. Ren, Y. Zhang, H. S. Peng, *J. Mater. Chem. A* **2015**, *3*, 10942.
[110] W. Weng, Q. Sun, Y. Zhang, H. J. Lin, J. Ren, X. Lu, M. Wang, H. S. Peng, *Nano Lett.* **2014**, *14*, 3432.
[111] J. Ren, Y. Zhang, W. Y. Bai, X. L. Chen, Z. T. Zhang, X. Fang, W. Weng, Y. G. Wang, H. S. Peng, *Angew. Chem., Int. Ed.* **2014**, *53*, 7864.
[112] H. Sun, Y. S. Jiang, S. L. Xie, Y. Zhang, J. Ren, A. Ali, S. G. Doo, I. H. Son, X. L. Huang, H. S. Peng, *J. Mater. Chem. A* **2016**, *4*, 7601.
[113] Y. Zhang, Y. H. Wang, L. Wang, C. M. Lo, Y. Zhao, Y. D. Jiao, G. F. Zheng, H. S. Peng, *J. Mater. Chem. A* **2016**, *4*, 9002.
[114] Y. B. Wang, C. J. Chen, H. Xie, T. T. Gao, Y. G. Yao, G. Pastel, X. G. Han, Y. J. Li, J. P. Zhao, K. Fu, L. B. Hu, *Adv. Funct. Mater.* **2017**, *27*, 1703140.
[115] T. Hoshide, Y. C. Zheng, J. Y. Hou, Z. Q. Wane, Q. W. Li, Z. G. Zhao, R. Z. Ma, T. Sasaki, F. X. Geng, *Nano Lett.* **2017**, *17*, 3543.
[116] Z. P. Wu, K. X. Liu, C. Lv, S. W. Zhong, Q. H. Wang, T. Liu, X. B. Liu, Y. H. Yin, Y. Y. Hu, D. Wei, Z. F. Liu, *Small* **2018**, *14*, 1800414.
[117] X. Fang, W. Weng, J. Ren, H. S. Peng, *Adv. Mater.* **2016**, *28*, 491.
[118] R. Q. Liu, Y. J. Liu, J. Chen, Q. Kang, L. L. Wang, W. X. Zhou, Z. D. Huang, X. J. Lin, Y. Li, P. Li, X. M. Feng, G. Wu, Y. W. Ma, W. Huang, *Nano Energy* **2017**, *33*, 325
[119] W. G. Chong, J. Q. Huang, Z. L. Xu, X. Y. Qin, X. Y. Wang, J. K. Kim, *Adv. Funct. Mater.* **2017**, *27*, 1604815.
[120] T. Liu, Q. C. Liu, J. J. Xu, X. B. Zhang, *Small* **2016**, *12*, 3101.
[121] Y. Zhang, L. Wang, Z. Y. Guo, Y. F. Xu, Y. G. Wang, H. S. Peng, *Angew. Chem., Int. Ed.* **2016**, *55*, 4487.
[122] J. Park, M. Park, G. Nam, J. S. Lee, J. Cho, *Adv. Mater.* **2015**, *27*, 1396.
[123] Y. F. Xu, Y. Zhang, Z. Y. Guo, J. Ren, Y. G. Wang, H. S. Peng, *Angew. Chem., Int. Ed.* **2015**, *54*, 15390.
[124] C. Tang, B. Wang, H. F. Wang, Q. Zhang, *Adv. Mater.* **2017**, *29*, 1703185.
[125] Y. F. Xu, Y. Zhao, J. Ren, Y. Zhang, H. S. Peng, *Angew. Chem., Int. Ed.* **2016**, *55*, 7979.
[126] Y. Zhang, Y. D. Jiao, L. J. Lu, L. Wang, T. Q. Chen, H. S. Peng, *Angew. Chem., Int. Ed.* **2017**, *56*, 13741.
[127] Y. H. Zhu, S. Yuan, D. Bao, Y. B. Yin, H. X. Zhong, X. B. Zhang, J. M. Yan, Q. Jiang, *Adv. Mater.* **2017**, *29*, 1603719.
[128] L. Li, Z. Wu, S. Yuan, X. B. Zhang, *Energy Environ. Sci.* **2014**, *7*, 2101.
[129] L. F. Cui, L. B. Hu, J. W. Choi, Y. Cui, *ACS Nano* **2010**, *4*, 3671.
[130] K. Fu, O. Yildiz, H. Bhanushali, Y. X. Wang, K. Stano, L. G. Xue, X. W. Zhang, P. D. Bradford, *Adv. Mater.* **2013**, *25*, 5109.
[131] K. Wang, S. Luo, Y. Wu, X. F. He, F. Zhao, J. P. Wang, K. L. Jiang, S. S. Fan, *Adv. Funct. Mater.* **2013**, *23*, 846.
[132] Q. Cheng, Z. M. Song, T. Ma, B. B. Smith, R. Tang, H. Y. Yu, H. Q. Jiang, C. K. Chan, *Nano Lett.* **2013**, *13*, 4969.
[133] Z. M. Song, T. Ma, R. Tang, Q. Cheng, X. Wang, D. Krishnaraju, R. Panat, C. K. Chan, H. Y. Yu, H. Q. Jiang, *Nat. Commun.* **2014**, *5*, 3140.
[134] T. Liu, M. Zhang, Y. L. Wang, Q. Y. Wang, C. Lv, K. X. Liu, S. Suresh, Y. H. Yin, Y. Y. Hu, Y. S. Li, X. B. Liu, S. W. Zhong, B. Y. Xia, Z. P. Wu, *Adv. Energy Mater.* **2018**, *8*, 1802349.
[135] C. Y. Wang, D. Li, C. O. Too, G. G. Wallace, *Chem. Mater.* **2009**, *21*, 2604.
[136] Z. Q. Niu, J. Chen, H. H. Hng, J. Ma, X. D. Chen, *Adv. Mater.* **2012**, *24*, 4144.
[137] Z. S. Wu, G. M. Zhou, L. C. Yin, W. Ren, F. Li, H. M. Cheng, *Nano Energy* **2012**, *1*, 107.
[138] L. Wen, F. Li, H. M. Cheng, *Adv. Mater.* **2016**, *28*, 4306.
[139] B. Liu, J. G. Zhang, G. Z. Shen, *Nano Today* **2016**, *11*, 82.
[140] S. M. Paek, E. Yoo, I. Honma, *Nano Lett.* **2009**, *9*, 72.
[141] Z. S. Wu, W. C. Ren, L. Wen, L. B. Gao, J. P. Zhao, Z. P. Chen, G. M. Zhou, F. Li, H. M. Cheng, *ACS Nano* **2010**, *4*, 3187.
[142] X. J. Zhu, Y. W. Zhu, S. Murali, M. D. Stollers, R. S. Ruoff, *ACS Nano* **2011**, *5*, 3333.
[143] D. H. Wang, D. W. Choi, J. Li, Z. G. Yang, Z. M. Nie, R. Kou, D. H. Hu, C. M. Wang, L. V. Saraf, J. G. Zhang, I. A. Aksay, J. Liu, *ACS Nano* **2009**, *3*, 907.
[144] Y. H. Ding, H. M. Ren, Y. Y. Huang, F. H. Chang, P. Zhang, *Mater. Res. Bull.* **2013**, *48*, 3713.
[145] H. Gwon, H. S. Kim, K. U. Lee, D. H. Seo, Y. C. Park, Y. S. Lee, B. T. Ahn, K. Kang, *Energy Environ. Sci.* **2011**, *4*, 1277.
[146] Y. Shi, L. Wen, G. M. Zhou, J. Chen, S. F. Pei, K. Huang, H. M. Cheng, F. Li, *2D Mater.* **2015**, *2*, 024004.
[147] N. Li, Z. P. Chen, W. C. Ren, F. Li, H. M. Cheng, *P. Nat. Proc. Natl. Acad. Sci. USA* **2012**, *109*, 17360.
[148] B. Liu, J. Zhang, X. F. Wang, G. Chen, D. Chen, C. W. Zhou, G. Z. Shen, *Nano Lett.* **2012**, *12*, 3005.
[149] M. S. Balogun, M. H. Yu, Y. C. Huan, C. Li, P. P. Fang, Y. Li, X. H. Lu, Y. X. Tong, *Nano Energy* **2015**, *11*, 348.
[150] J. F. Ruan, T. Yuan, Y. P. Pang, X. B. Xu, J. H. Yang, W. B. Hu, C. Zhong, Z. F. Ma, X. X. Bi, S. Y. Zheng, *ACS Appl. Mater. Interfaces* **2017**, *9*, 36261.
[151] S. Y. Chu, Y. J. Zhong, R. Cai, Z. B. Zhang, S. Y. Wei, Z. P. Shao, *Small* **2016**, *12*, 6724.
[152] M. Du, K. Rui, Y. Q. Chang, Y. Zhang, Z. Y. Ma, W. P. Sun, Q. Yan, J. X. Zhu, W. Huang, *Small* **2017**, *13*, 1702770.
[153] C. Kang, R. Baskaran, J. Hwang, B. C. Ku, W. Choi, *Carbon* **2014**, *68*, 493.
[154] R. W. Mo, D. Rooney, K. N. Sun, H. Y. Yang, *Nat. Commun.* **2016**, *8*, 13949.
[155] X. H. Wang, L. M. Sun, R. A. Susantyoko, Q. Zhang, *Carbon* **2016**, *98*, 504.
[156] L. L. Wang, D. Chen, K. Jiang, G. Z. Shen, *Chem. Soc. Rev.* **2017**, *46*, 6764.
[157] S. Yoon, S. Lee, S. Kim, K. W. Park, D. Cho, Y. Jeong, *J. Power Sources* **2015**, *279*, 495.
[158] X. Fang, C. F. Shen, M. Y. Ge, J. P. Rong, Y. H. Liu, A. Y. Zhang, F. Wei, C. W. Zhou, *Nano Energy* **2015**, *12*, 43.
[159] M. H. Park, M. Noh, S. Lee, M. Ko, S. Chae, S. Sim, S. Choi, H. Kim, H. Nam, S. Park, J. Cho, *Nano Lett.* **2014**, *14*, 4083.
[160] H. P. Wu, Q. H. Meng, Q. Yang, M. Zhang, K. Lu, Z. X. Wei, *Adv. Mater.* **2015**, *27*, 6504.
[161] F. X. Wu, E. B. Zhao, D. Gordon, Y. R. Xiao, C. C. Hu, G. Yushin, *Adv. Mater.* **2016**, *28*, 6365.
[162] M. Li, W. Wahyudi, P. Kumar, F. Wu, X. Yang, H. Li, L. J. Li, J. Ming, *ACS Appl. Mater. Interfaces* **2017**, *9*, 8047.
[163] H. L. Wang, Y. Yang, Y. Y. Liang, J. T. Robinson, Y. G. Li, A. Jackson, Y. Cui, H. J. Dai, *Nano Lett.* **2011**, *11*, 2644.
[164] G. M. Zhou, L. Li, D. W. Wang, X. Y. Shan, S. F. Pei, F. Li, H. M. Cheng, *Adv. Mater.* **2015**, *27*, 641.
[165] P. T. Xiao, F. X. Bu, G. H. Yang, Y. Zhang, Y. X. Xu, *Adv. Mater.* **2017**, *29*, 1703324.
[166] L. Li, Z. P. Wu, H. Sun, D. M. Chen, J. Gao, S. Suresh, P. Chow, C. V. Singh, N. Koratkar, *ACS Nano* **2015**, *9*, 11342.
[167] Y. Y. Mao, G. R. Li, Y. Guo, Z. P. Li, C. D. Liang, X. S. Peng, Z. Lin, *Nat. Commun.* **2017**, *8*, 14628.
[168] J. Lim, J. Pyun, K. Char, *Angew. Chem., Int. Ed.* **2015**, *54*, 3249.

[169] J. T. Hughes, D. F. Sava, T. M. Nenoff, A. Navrotsky, *J. Am. Chem. Soc.* **2013**, *135*, 16256.
[170] M. W. Xiang, H. Wu, H. Liu, J. Huang, Y. F. Zheng, L. Yang, P. Jing, Y. Zhang, S. X. Dou, H. K. Liu, *Adv. Funct. Mater.* **2017**, *27*, 1702573.
[171] C. Lin, C. J. Niu, X. Xu, K. Li, Z. Y. Cai, Y. L. Zhang, X. P. Wang, L. B. Qu, Y. X. Xu, L. Q. Mai, *Phys. Chem. Chem. Phys.* **2016**, *18*, 22146.
[172] Z. Q. Lin, Z. P. Zeng, X. C. Gui, Z. K. Tang, M. C. Zou, A. Y. Cao, *Adv. Energy Mater.* **2016**, *6*, 1600554.
[173] Y. L. Li, J. J. Wang, X. F. Li, D. S. Geng, R. Y. Li, X. L. Sun, *Chem. Commun.* **2011**, *47*, 9438.
[174] B. Sun, X. D. Huang, S. Q. Chen, P. Munroe, G. X. Wang, *Nano Lett.* **2014**, *14*, 3145.
[175] Q. C. Liu, L. Li, J. J. Xu, Z. W. Chang, D. Xu, Y. B. Yin, X. Y. Yang, T. Liu, Y. S. Jiang, J. M. Yan, X. B. Zhang, *Adv. Mater.* **2015**, *27*, 8095.
[176] Q. C. Liu, J. J. Xu, D. Xu, X. B. Zhang, *Nat. Commun.* **2015**, *6*, 7892.
[177] Q. C. Liu, T. Liu, D. P. Liu, Z. J. Li, X. B. Zhang, Y. Zhang, *Adv. Mater.* **2016**, *28*, 8413.
[178] Y. X. Jiang, J. F. Cheng, L. Zou, X. Y. Li, Y. Z. Huang, L. C. Jia, B. Chi, J. Pu, J. Li, *ChemCatChem* **2017**, *9*, 4231.
[179] T. Liu, J. J. Xu, Q. C. Liu, Z. W. Chang, Y. B. Yin, X. Y. Yang, X. B. Zhang, *Small* **2017**, *13*, 1602952.
[180] X. F. Hu, Z. F. Li, J. Chen, *Angew. Chem., Int. Ed.* **2017**, *56*, 5785.
[181] Y. X. Hu, D. L. Ye, B. Luo, H. Hu, X. B. Zhu, S. C. Wang, L. L. Li, S. J. Peng, L. Z. Wang, *Adv. Mater.* **2017**, *29*, 1703824.
[182] Y. H. Liu, A. Y. Zhang, C. F. Shen, Q. Z. Liu, X. A. Cao, Y. Q. Ma, L. A. Chen, C. Lau, T. C. Chen, F. Wei, C. W. Zhou, *ACS Nano* **2017**, *11*, 5530.
[183] H. R. An, Y. Li, Y. Gao, C. Cao, J. K. Han, Y. Y. Feng, W. Feng, *Carbon* **2017**, *116*, 338.
[184] L. David, R. Bhandavat, G. Singh, *ACS Nano* **2014**, *8*, 1759.
[185] Y. Yao, L. C. Zeng, S. H. Hu, Y. Jiang, B. B. Yuan, Y. Yu, *Small* **2017**, *13*, 1602952.
[186] Q. Liu, Y. B. Wang, L. M. Dai, J. N. Yao, *Adv. Mater.* **2016**, *28*, 3000.
[187] P. Hiralal, S. Imaizumi, H. E. Unalan, H. Matsumoto, M. Minagawa, M. Rouvala, A. Tanioka, G. A. J. Amaratunga, *ACS Nano* **2010**, *4*, 2730.
[188] K. K. Fu, J. Cheng, T. Li, L. B. Hu, *ACS Energy Lett.* **2016**, *1*, 1065.
[189] M. B. Bryning, D. E. Milkie, M. F. Islam, L. A. Hough, J. M. Kikkawa, A. G. Yodh, *Adv. Mater.* **2007**, *19*, 661.
[190] P. X. Li, C. Y. Kong, Y. Y. Shang, E. Z. Shi, Y. T. Yu, W. Z. Qian, F. Wei, J. Q. Wei, K. L. Wang, H. W. Zhu, A. Y. Cao, D. H. Wu, *Nanoscale* **2013**, *5*, 8472.
[191] X. P. Cheng, X. C. Gui, Z. Q. Lin, Y. J. Zheng, M. Liu, R. Z. Zhan, Y. Zhu, Z. K. Tang, *J. Mater. Chem. A* **2015**, *3*, 20927.
[192] M. Xu, D. N. Futaba, M. Yumura, K. Hata, *Nano Lett.* **2011**, *11*, 3279.
[193] X. Y. Chen, H. L. Zhu, Y. C. Chen, Y. Y. Shang, A. Y. Cao, L. B. Hu, G. W. Rubloff, *ACS Nano* **2012**, *6*, 7948.
[194] C. S. Shan, W. J. Zhao, X. L. Lu, D. J. O'Brien, Y. P. Li, Z. Y. Cao, A. L. Elias, R. Cruz-Silva, M. Terrones, B. Q. Wei, *Nano Lett.* **2013**, *13*, 5514.
[195] Y. Liu, W. Z. Qian, Q. Zhang, A. Y. Cao, Z. F. Li, W. P. Zhou, Y. Ma, F. Wei, *Nano Lett.* **2008**, *8*, 1323.
[196] Q. Zhang, M. Q. Zhao, Y. Liu, A. Y. Cao, W. Z. Qian, Y. F. Lu, F. Wei, *Adv. Mater.* **2009**, *21*, 2876.
[197] H. S. Peng, X. M. Sun, F. J. Cai, X. L. Chen, Y. C. Zhu, G. P. Liao, D. Y. Chen, Q. W. Li, Y. F. Lu, Y. T. Zhu, Q. X. Jia, *Nat. Nanotechnol.* **2009**, *4*, 738.
[198] P. N. Chen, Y. F. Xu, S. S. He, X. M. Sun, S. W. Pan, J. Deng, D. Y. Chen, H. S. Peng, *Nat. Nanotechnol.* **2015**, *10*, 1077.
[199] Z. T. Zhang, K. P. Guo, Y. M. Li, X. Y. Li, G. Z. Guan, H. P. Li, Y. F. Luo, F. Y. Zhao, Q. Zhang, B. Wei, Q. B. Pei, H. S. Peng, *Nat. Photonics* **2015**, *9*, 233.